

Crowd-Anticrowd Theory of Multi-Agent Minority Games

Michael L. Hart and Neil F. Johnson*

Physics Department, Oxford University, Oxford, OX1 3PU, UK

February 2, 2019

Abstract

We present a formal treatment of the Crowd-Anticrowd theory of Minority Games played by a population of competing agents. This theory is built around a description of the crowding which arises within the game's strategy space. Earlier works have shown that this theory provides a simple, yet quantitatively accurate explanation of the time-averaged behavior of these multi-agent games. We also discuss the extent to which the Crowd-Anticrowd approach provides a useful tool for analyzing a wider class of Complex Systems.

*n.johnson@physics.ox.ac.uk

1 Introduction

The now-famous Minority Game (MG) was introduced by Challet and Zhang [1] as a means of simplifying Brian Arthur’s original El Farol Bar Problem [2, 3]. The fascination with the MG among researchers from physics, computer science, biology and economics, has led to the appearance of more than one hundred MG-related papers within the past few years (see, for example, Refs. [4, 5, 6, 7, 8, 9, 10, 11, 12, 13, 14, 15, 16, 17, 18, 20, 21, 22, 23, 24, 25, 26, 27, 28, 29, 30, 31]). A detailed list, with informative comments by Damien Challet, is available from Ref. [32]. The game itself concerns a population of N heterogeneous agents with limited capabilities and information, who repeatedly compete to be in the minority group. The agents (e.g. people, cells, data-packets) are adaptive, but only have access to global information about the game’s progress.

The numerical results obtained by Savit and co-workers [13] prompted widespread interest in the Minority Game. These results showed that the time-averaged fluctuations in the game’s output – or equivalently, the time-averaged fluctuations in wastage of the underlying global resource – vary in a highly non-linear fashion as a function of the memory m of the agents. Reference [16] provided the first explanation of this ‘Savit curve’. In particular it was shown that the formation of, and competition between, crowds and anticrowds can explain both qualitatively and quantitatively the Savit curve for the basic MG [16, 17]. In addition, the Crowd-Anticrowd approach has been shown to describe the fluctuations within more general MGs: for example, an MG comprising a population of agents with different memories m [18, 19], an MG with stochastic strategy-use [20], and an MG with a mixed population of stochastic and non-stochastic strategy-use [21]. The task of fully understanding the MG is seen as an important stepping stone toward the development of a ‘Theory of Complex Systems’. Many systems have been proposed as real-world examples of the MG, in fields as diverse as biology, computing science, sociology, economics and finance. (Note however that the basic MG lacks the crucial feature present in financial markets whereby agents can sit out of the game and hence do nothing at any given timestep. Including this effect yields the Grand Canonical Minority Game (GCMG) as discussed in Refs. [19, 22], which can indeed show financial market-like behavior).

In addition to the Crowd-Anticrowd approach, there have been various more recent attempts to develop a quantitative theory which describes the fluctuations as a function of m in the MG [5, 6, 7, 8, 9, 11, 27, 28, 30, 31]. Although elegant and sophisticated, such theories have not been able to reproduce the numerical results of Ref. [13] over the full range of m . We believe that what is missing from such theories is an accurate description of the correlations between agents’ strategies: these correlations produce a highly-correlated form of decision noise which cannot then be easily averaged over or added in. By contrast these strong inter-strategy correlations take center-stage in the Crowd-Anticrowd theory.

The Crowd-Anticrowd approach is not limited to MG-like games. It is built around the effects of crowding (i.e. correlations) in strategy-space, rather than the precise rules of the game itself, and only makes fairly modest assumptions about a game’s dynamical behavior. Specifically, its

validity depends on the histories of the game (see Sec. 2) being visited reasonably frequently. As a result, it is likely that it is applicable to other forms of multi-agent game. To the extent that a given Complex System’s dynamics mimic such a multi-agent game, it is likely that the Crowd-Anticrowd approach will be applicable. This would be a welcome development, given the lack of general concepts in the field of Complex Systems as a whole. It is therefore important to lay out the theoretical framework underlying the theory, before proceeding with any broader investigations.

Despite the potential usefulness of the Crowd-Anticrowd theory, the formal derivation has not yet been presented in the literature. This observation motivates the present paper. The layout of the paper is as follows. For completeness, Section 2 provides a description of the basic MG. Section 3 presents a derivation of the Crowd-Anticrowd theory, while Section 4 looks at various limiting cases. The conclusion is given in Section 5.

2 Description of the Minority Game

Figure 1 summarizes the Minority Game (MG). At timestep t , each agent (e.g. a bar customer, a commuter, or a market trader) decides whether to enter a game where the choices are option 1 (e.g. attend the bar, take route A, or buy) and option 0 (e.g. go home, take route B, or sell). A total of $n_0(t)$ agents choose 0 while $n_1(t)$ choose 1. We can define an excess demand or net ‘attendance’ as

$$A(t) = n_1(t) - n_0(t). \quad (1)$$

The only global information available to the agents is a common memory of the recent history, i.e. the most recent m winning decisions/outcomes. For $m = 2$, these will have the form 00, 01, 10 or 11. Hence at each timestep, the recent history constitutes a particular bit-string. For general m , there will be $P = 2^m$ possible history bit-strings. These history bit-strings can alternatively be represented in decimal form: $\mu = \{0, 1, \dots, P-1\}$ where $\mu = 0$ corresponds to 00, $\mu = 1$ corresponds to 01 etc. A strategy consists of a response, 0 or 1, to each possible history bit-string. Hence there are 2^P possible strategies. For $m = 2$ for example, there are therefore 16 possible strategies. Each agent randomly picks s strategies at the outset of the game. The agents update the scores of their strategies after each timestep with $+1$ (or -1) as the pay-off for choosing the winning (or losing) action. Agents play their highest scoring strategy. If an agent holds two or more strategies that are tied for the position of ‘highest scoring strategy’ then the agent will use a fair random process (e.g. a coin-toss) to decide which of these strategies to use for that turn of the game.

A feature of the MG which has attracted much interest, is the standard deviation (or ‘volatility’) of the number of agents choosing a particular option over time, i.e. the standard deviation of $n_0(t)$ or $n_1(t)$ [13]. The time-averages of $n_0(t)$ and $n_1(t)$ are both approximately $N/2$ since neither 0 nor 1 is preferred as an outcome a priori. Only those agents who choose the correct minority option at a given turn get positively rewarded, hence

the standard deviation of $n_0(t)$ or $n_1(t)$ (and $A(t)$) indicates the level of wastage in the system. If the standard deviation of $n_0(t)$ is small then a relatively large proportion of agents are getting rewarded positively at each timestep, and hence the level of wastage $|n_0(t) - N/2|$ is small. Conversely, if the standard deviation of $n_0(t)$ is large then a relatively small proportion of agents are getting rewarded positively at each timestep, and hence the level of wastage $|n_0(t) - N/2|$ is large.

Figure 2 shows the ‘Savit curve’. This plots the standard deviation (i.e. volatility) of agents choosing a particular option, as a function of memory size m . The numerical values are shown as small circles, and were obtained from individual simulation runs. The data for each run is collected once initial transient effects have settled down. The volatilities from different runs differ because of different initial strategy allocations among the agents, and different outcomes from the coin-tosses used to break ties in strategy scores. The dashed line represents the volatility one would get if all the agents used the toss of a coin to decide which option to choose at every timestep. To see how this is calculated, consider the case of N independent agents each deciding which option to choose by the toss of a coin. Each agent therefore provides a random-walk process in terms of increasing or decreasing $A(t)$ by 1. Assume for the moment that these coin-tosses are uncorrelated. Then the total variance of this random-walk in the attendance $A(t)$, is given by the sum of the individual variances produced by each of the N agents. If the agent decides 1, then he contributes 1 to the attendance $A(t)$. [The random-walk “step-size” is $d = 1$]. If, by contrast, the agent decides 0, then he contributes -1 to the attendance $A(t)$. The agent chooses 1 with probability $p = 1/2$, and 0 with probability $q = 1/2$. The variance contributed to σ^2 by each agent is therefore given by the random-walk result $4pqd^2 = 1$. Summing over all N agents, the total variance in the excess demand is given by $4Npqd^2 = N$. The variance σ_1^2 of $n_1(t)$ can be obtained from the variance σ^2 of $A(t)$ by dividing by a factor 4 [since $2\sigma_1 = \sigma$]. Hence the variance σ_1^2 of $n_1(t)$ is given by $N/4$. The corresponding standard deviation $\sigma_1 = \sqrt{N}/2$ is the dashed ‘coin-toss’ line in the plot (i.e. $\sigma_1 \approx 5.0$ for $N = 101$). The solid lines in Figure 2 correspond to analytic Crowd-Anticrowd results calculated in various regimes: these are discussed later in the paper.

2.1 Strategy Space

A strategy is defined as a set of instructions to describe what an agent should do in any given situation, i.e. given any particular history μ the strategy decides what the agent should do. The strategy space is the set of strategies from which agents are allocated their strategies at the beginning of the game. Any strategy in the strategy space can in principle be present in the game: however if a strategy is not in the set which is initially allocated, then it can never appear in that particular run of the MG game. Figure 3 shows an $m = 2$ strategy space together with some example strategies. The strategy space shown is known as the ‘Full Strategy Space’, FSS, and contains all possible permutations of the binary options 0 and 1 for each history. As such there are 2^{2^m} strategies in this space. The 2^m dimensional hypercube shows all 2^{2^m} strategies from the

full strategy space at its vertices. It is clear that the agents playing the game are limited by the set of strategies that they are allocated at the start of the game. (This initial strategy-allocation is random). Of course there are many more strategies that can be thought of, but which aren't present within the FSS. For example, the simple strategies of persistence and anti-persistence are not present in the FSS. The advantage however of using the FSS in the MG is that the strategies form a complete set and as such display no bias towards any option given a history. There are also practical reasons for using a binary strategy space. Consider a game with a memory size of $m = 8$, i.e. the agents can look at the last 8 outcomes of the game to decide what to do next. Even with binary options for a given history there are a large number of strategies – in particular there are $2^{2^m} = 1.16 \times 10^{77}$. To include any additional strategies like persistence and anti-persistence would mean opening up the strategy space, hence losing the simplicity of the MG and returning to the complexity of Arthur's original Bar Problem [2, 3].

2.2 Reduced Strategy Space (RSS)

It can be observed from the FSS, that one can choose a subset of strategies [4] such that any pair within this subset has one of the following characteristics:

- anti-correlated, e.g. 0000 and 1111. For example, any two agents using the ($m = 2$) strategies 0000 and 1111 respectively, would take the opposite action irrespective of the sequence of previous outcomes and hence the history. Hence one agent will always do the opposite of the other agent. For example, if one agent buys at a given timestep, the other agent will sell. Their net effect on the attendance $A(t)$ therefore cancels out at each timestep. Hence they will not contribute to fluctuations in $A(t)$. In short they do not contribute to the volatility. This is a crucial observation for understanding the behaviour of the volatility in this system, as we discuss later on.
- uncorrelated, e.g. 0000 and 0011. For example, any two agents using the strategies 0000 and 0011 respectively, would take the opposite action for two of the four histories, while they would take the same action for the remaining two histories. Assuming that the $m = 2$ histories occur equally often, the actions of the two agents will be uncorrelated on average.

A convenient measure of the distance (i.e. closeness) of any two strategies is the Hamming distance which is defined by the number of bits that need to be changed in going from one strategy to another. For example, the Hamming distance between 0000 and 1111 is 4, while the Hamming distance between 0000 and 0011 is just 2. Although there are $2^P \equiv 2^{2^{m=2}} \equiv 16$ strategies in the $m = 2$ strategy space, it can be seen that one can choose subsets such that any strategy-pair within this subset is either anti-correlated or uncorrelated. Consider, for example, the two groups

$$U_{m=2} \equiv \{0000, 1100, 1010, 0110\}$$

and

$$\overline{U_{m=2}} \equiv \{1111, 0011, 0101, 1001\}.$$

Any two strategies within $U_{m=2}$ are uncorrelated since they have a Hamming distance of 2. Likewise any two strategies within $\overline{U_{m=2}}$ are uncorrelated since they have a relative Hamming distance of 2. However, each strategy in $U_{m=2}$ has an anti-correlated strategy in $\overline{U_{m=2}}$: for example, 0000 is anti-correlated to 1111, 1100 is anti-correlated to 0011 etc. This subset of strategies comprising $U_{m=2}$ and $\overline{U_{m=2}}$, forms a Reduced Strategy Space (RSS) [4]. Since it contains the essential correlations of the Full Strategy Space (FSS), it turns out that running the simulation within the RSS reproduces the main features of the full game obtained using the FSS [4]. The RSS has a smaller number of strategies $2 \cdot 2^m = 2P \equiv 2^{m+1}$ than the FSS which has $2^P = 2^{2^m}$. For $m = 2$, there are 8 strategies in the RSS, compared to 16 in the FSS, whilst for $m = 8$ there are 1.16×10^{77} strategies in the FSS, but only 512 strategies in the RSS. We note that the choice of the RSS is not unique, i.e. within a given FSS there are many possible choices for a RSS. In particular, it is possible to create $2^{2^m} / 2^{m+1}$ distinct reduced strategy spaces from the FSS. To summarize, the RSS provides a minimal set of strategies which ‘span’ the FSS and are hence representative of its full structure.

2.3 History Space: de Bruijn graph

The history μ of recent outcomes changes in time, i.e. it is a dynamical variable. Interestingly the dynamics of this history can be represented on a directed graph (a so-called digraph). The particular form of directed graph is called a de Bruijn graph. Figure 4 shows some examples of the de Bruijn graph for $m = 1, 2$, and 3. The probability that the outcome at time $t + 1$ will be a 1 (or 0) depends on the state at time t . Hence it will depend on the previous m outcomes, i.e. it depends on the particular state of the history bit-string. The dependence on earlier timesteps means that the game is non-Markovian. We note that modifying the game to a finite time-horizon for scoring strategies, allows the resulting game to be viewed as a high-dimensional Markov process [23, 24]. However, here we focus on the basic MG where scores are kept from the beginning of the game.

2.4 Initial conditions for the MG

The dynamics for a particular run of the game depend upon the strategies that the agents are initially assigned and the random process used to decide tie-breaks. The particular dynamics which emerge also depend upon the initial score-vector of the strategies and initial history used to seed the start of the game. If the initial strategy score-vector is not ‘typical’, then a bias can be introduced into the game which never disappears. In short, the system never recovers from this bias. It will be assumed that no such initial bias exists. In practice this is achieved, for example, by setting all the initial scores to zero. The initial choice of history is not considered to be an important effect. It is assumed that any transient effects resulting from the particular history seed will have disappeared, i.e.

the initial history seed does not introduce any long-term bias. A typical game is left to run for over 10,000 timesteps such that any transients are washed out of the system.

The initial strategy allocation among agents can be described in terms of a tensor Ω [25]. This tensor Ω describes the distribution of strategies among the N individual agents and hence the particular *quenched disorder* of the system. The dimension of Ω is given by the number of strategies s that each agent holds. For example, for $s = 3$ the element $\Omega_{i,j,k}$ gives the number of agents assigned strategy i , then strategy j , and then strategy k , in that order. Hence

$$\sum_{i,j,k,\dots}^D \Omega_{i,j,k,\dots} = N, \quad (2)$$

where the value of D represents the number of distinct strategies that exist within the strategy space chosen. $D = 2^{2^m}$ in the FSS, whilst $D = 2.2^m$ in the RSS. Figure 5 shows an example distribution Ω for $N = 101$ agents in the case of $m = 2$, and $s = 2$ in the reduced strategy space RSS. We note that while Ω is not symmetric, it could be made so since the MG does not distinguish between the order in which the two strategies are picked.

3 Derivation of Crowd-Anticrowd theory

3.1 Qualitative explanation

We start by providing a qualitative explanation of the ‘Savit curve’ in Figure 2 (small circles). Our explanation is based on the RSS, but we note that Figure 2 is practically identical for both RSS and FSS. First we introduce the notion of *crowd* and *anticrowd*. Consider a group of agents whose highest-scoring strategy is R over δt timesteps. This group constitutes a *crowd* since they all use this same strategy R and hence act in the same way for those δt timesteps *regardless* of the particular history bit-string at each timestep. Next consider the group of agents whose highest-scoring strategy over the same τ timesteps is the anti-correlated partner to R , which we refer to as \bar{R} . This group constitutes an *anticrowd* with respect to the crowd using strategy R , since they will act in the opposite way to the first crowd at each timestep *regardless* of the particular history bit-string.

Figure 6 indicates the competition between crowd-anticrowd sizes which arises as a function of m . The curve in the upper graph shows the volatility from Figure 2 averaged over runs, as a function of m . The low- m phase, characterized by a decrease in σ as m increases, is called the crowded phase since the number of strategies in the RSS 2^{m+1} is small compared to the number of agents N . The high- m phase, characterized by a slow increase in σ towards a limiting value as m increases, is called the dilute phase since the number of strategies in the RSS 2^{m+1} is now large compared to the number of agents N .

In the crowded phase, i.e. at small m , there will at any one time be a large number of agents who are using a given strategy R and so will

flood into the market as a crowd. Although the crowd may maintain strategy R for several timesteps, the resulting outcome will tend to flip between 0 and 1 in response to the changing history bit-string (consider, for example, strategy 0011 which produces equal numbers of 0's and 1's as the game cycles through history bit-strings). This gives rise to a high volatility. Eventually, strategy R will lose enough points to be deemed a bad strategy by many of the crowd members. Hence the crowd using a given strategy R is continually changing its membership and size. We emphasize that the crowding effect we are discussing at any given timestep will occur *regardless* of the actual history bit-string at that timestep, since it is a crowding effect in strategy space rather than merely a crowding in terms of eventual action. In other words, we are not just making the trivial statement that a crowd comprises agents who act in the same way at a given timestep – instead we are saying that a crowd is characterized by agents who all believe that a given strategy is the best, and will therefore take the same action regardless of the history bit-string at a particular timestep.

As the memory m of the agents increases, the number of agents using high-scoring strategies tends to decrease simply because many may not now possess such strategies. This implies a decrease in the crowd-sizes, but an increase in the number of crowds reflecting an increase in the number of strategies available. There will also be groups of agents who are forced to use the anti-correlated (i.e. low-scoring) strategies. The actions of these anticrowds will cancel out the action of the crowds. This argument applies to all pairs of anti-correlated strategies, i.e. the crowd-anticrowd pair corresponding to the best/worst strategy pair, the crowd-anticrowd pair corresponding to the second-best/second-worst strategy pair, etc. As m increases, the crowd-sizes decrease while the anticrowd sizes increase: this yields an increase in the crowd-anticrowd cancellation effect and hence a reduction in the size of the volatility. Eventually in the dilute phase of very large memory m , it is very unlikely that any agents will use (or even hold) the same strategies. It is also unlikely that any two agents will be using anti-correlated strategies. Hence the crowd-anticrowd cancellation is reduced, thereby increasing the volatility. Because of the lack of correlated groups (i.e. all crowds and anticrowds are of size 1 or 0) the volatility can now be modelled by assuming that the population comprises independent, coin-tossing agents.

We now add some analytics to this verbal description. Consider the crowd of agents n_R using a particular strategy R at a particular moment during the game, and the anticrowd of $n_{\bar{R}}$ agents who are using the anticorrelated strategy to R . Over the timescale during which the two opposing strategies are being played, the fluctuations are determined only by the net crowd-size $n_R^{eff} = n_R - n_{\bar{R}}$ which constitutes the net step-size of the crowd-anticrowd pair in a random-walk model for the attendance. The net contribution to the volatility by this crowd-anticrowd pair is therefore $pqd^2 = [n_R^{eff}]^2/4$. This simple expression enables us to discuss the order of magnitude of the volatility within the three main regions of the curve seen in Figure 2:

- $2^{m+1} \ll N.s$: suppose strategy R^* is the highest scoring at a

particular moment. The anti-correlated strategy \overline{R}^* is therefore the lowest scoring at that same moment. In the limit of small m , the size of the strategy space is small. Each agent hence carries a considerable fraction of all possible strategies. Therefore, even if an agent picks \overline{R}^* among his s strategies, he is also likely to have a high scoring strategy. Therefore, many agents will choose to use either R^* itself (if they hold it) or a similar one. In this regime the crowd associated with the highest-scoring strategies will dominate. Therefore $n_R \sim N\delta_{RR^*}$ and hence $n_R^{eff} \sim N\delta_{RR^*}$. This implies that the variance varies as $N^2/4$, i.e. the volatility is $\sigma \sim N/2 = 50$ for $N = 101$.

- $2^{m+1} \gg N.s$: in the limit of large m , the strategy space is very large and agents will have a low chance of holding the same strategy. Even if an agent has several low-scoring strategies, the probability of his best strategy being strictly anticorrelated to another agent's best strategy (hence forming a crowd-anticrowd pair) is small. All the crowds and anticrowds will tend to be of size 1 or 0, hence there are of order N contributions to the variance, each with effective step-size $n_R^{eff} = 1$. This implies that the variance varies as $N[n_R^{eff}]^2/4 = N/4$, i.e. the volatility is $\sigma \sim \sqrt{N}/2 = 5$ for $N = 101$.
- $2^{m+1} \sim N.s$: in the intermediate m region where the numerical minimum exists, the size of the strategy space is relatively large. Hence some agents may get stuck with s strategies which are all low scoring. They hence form anticrowds. Considering the extreme case where the crowd and anticrowd are of similar size, this gives $n_R^{eff} \sim 0$ and hence the volatility $\sigma \rightarrow 0$. For a fixed value of m , this regime of small volatility will arise for small s since, in this case, the number of strategies available to each agent is small - hence some of the agents may indeed be forced to use a strategy which is little better than the poorly-performing \overline{R}^* . In other words, the cancellation effect of the crowd and anticrowd becomes most effective in this intermediate region for small s . Increasing s will make this minimum less marked since it will reduce the number of agents forced to use the anti-correlated strategy, hence reducing the crowd-anticrowd cancellation effect in the volatility (as shown later in Figure 11).

We note that this Crowd-Anticrowd concept, and the subsequent detailed theory presented below, does not use any knowledge of the specific history bit-string at a given time-step. Hence the theory does not depend on the detailed dynamics of the history bit-string, as long as the dynamics is such that all histories (i.e. nodes in the de Bruijn graph) are visited frequently thereby guaranteeing that the measure of correlation for strategy pairs will have meaning. Hence the crowd-anticrowd theory would predict the same volatility for the MG regardless of whether the real history was used at each timestep, or whether it was replaced by a random bit-string. This is indeed what has been found in numerical studies of the volatility by Cavagna [29], thereby establishing the usefulness of the Crowd-Anticrowd approach.

3.2 Proof of concept

Having given a qualitative understanding of the underlying physics, we now provide a numerical proof-of-concept of the Crowd-Anticrowd approach before giving a formal derivation of the theory itself. Consider a given realization of the quenched disorder Ω and a timestep t in a given run for this given Ω . There is a current score-vector $\underline{S}[t]$ and a current history $\mu[t]$ which define the state of the game. The attendance $A(t) = A[\underline{S}[t], \mu[t]]$ is given by Equation 1. The volatility for a given run corresponds to a *time-average*: it is the standard deviation of the number of agents making a given decision (e.g. 1) for a given realization of the quenched disorder Ω and a given set of initial conditions. The volatility will eventually be averaged over many runs, each having their own strategy allocations, and hence will effectively be averaged over all realizations of the quenched disorder Ω and all sets of initial conditions. However, we first focus on a *given* realization of the quenched disorder Ω . We will assume that the quantities of interest (i.e. the mean and standard deviation of the attendance $A(t)$, and hence also $n_1(t)$ and $n_0(t)$) self-average for a given realization of the quenched disorder Ω . In other words, it is assumed that the average over time is equivalent to an average over initial conditions for the given realization of the quenched disorder Ω . We have checked using numerical simulations that this assumption is valid.

The attendance in Equation 1 can be rewritten by summing over the RSS as follows:

$$A[\underline{S}[t], \mu[t]] = n_1(t) - n_0(t) \equiv \sum_{R=1}^{2^P} a_R^{\mu[t]} n_R^{\underline{S}[t]}, \quad (3)$$

where $P = 2^m$ and the quantity $a_R^{\mu[t]}$ is the response of strategy R to the history bit-string μ at time t . Option 1 corresponds to $a_R^{\mu[t]} = 1$ while option 0 corresponds to $a_R^{\mu[t]} = -1$. The quantity $n_R^{\underline{S}[t]}$ is the number of agents using strategy R at time t . [The superscript $\underline{S}[t]$ is a reminder that this number of agents will depend on the strategy score at time t]. The calculation of the average attendance will now be shown, where the average is over time for a given realization of the quenched disorder Ω . $\langle X(t) \rangle_t$ is defined as a time-average over the variable $X(t)$ for a given Ω . By assuming the self-averaging property for a given Ω , the system is essentially assumed to be ergodic: hence we can assume that all histories

will be visited with similar frequency in a given run. Hence

$$\begin{aligned}
\langle A [\underline{S}[t], \mu[t]] \rangle_t &= \sum_{R=1}^{2P} \left\langle a_R^{\mu[t]} n_R^{\underline{S}[t]} \right\rangle_t \\
&= \sum_{R=1}^{2P} \left\langle a_R^{\mu[t]} \right\rangle_t \left\langle n_R^{\underline{S}[t]} \right\rangle_t \\
&= \sum_{R=1}^{2P} \left(\frac{1}{P} \sum_{\mu=0}^{P-1} a_R^{\mu[t]} \right) \left\langle n_R^{\underline{S}[t]} \right\rangle_t \\
&= \sum_{R=1}^{2P} 0 \cdot \left\langle n_R^{\underline{S}[t]} \right\rangle_t \\
&= 0.
\end{aligned} \tag{4}$$

Notice that the averaging is performed over all the histories, because of the ergodic assumption. The interest is in the *fluctuations* of $A(t)$ about this average value. Hence the volatility of $A(t)$ is considered. The variance (or volatility squared) is given by

$$\begin{aligned}
\sigma_\Omega^2 &= \langle A [\underline{S}[t], \mu[t]]^2 \rangle_t - \langle A [\underline{S}[t], \mu[t]] \rangle_t^2 \\
&= \langle A [\underline{S}[t], \mu[t]]^2 \rangle_t \\
&= \sum_{R, R'=1}^{2P} \left\langle a_R^{\mu[t]} n_R^{\underline{S}[t]} a_{R'}^{\mu[t]} n_{R'}^{\underline{S}[t]} \right\rangle_t.
\end{aligned} \tag{5}$$

This double sum is now broken into three parts: $\underline{a_R} \cdot \underline{a_{R'}} = P$ (correlated), $\underline{a_R} \cdot \underline{a_{R'}} = -P$ (anti-correlated), and $\underline{a_R} \cdot \underline{a_{R'}} = 0$ (uncorrelated). While this cannot be done in the FSS, the decomposition is exact in the RSS. Hence we have

$$\begin{aligned}
\sigma_\Omega^2 &= \sum_{R=1}^{2P} \left\langle \left(a_R^{\mu[t]} \right)^2 \left(n_R^{\underline{S}[t]} \right)^2 \right\rangle_t + \sum_{R=1}^{2P} \left\langle a_R^{\mu[t]} a_{\bar{R}}^{\mu[t]} n_R^{\underline{S}[t]} n_{\bar{R}}^{\underline{S}[t]} \right\rangle_t + \sum_{R \neq R' \neq \bar{R}}^{2P} \left\langle a_R^{\mu[t]} a_{R'}^{\mu[t]} n_R^{\underline{S}[t]} n_{R'}^{\underline{S}[t]} \right\rangle_t \\
&= \sum_{R=1}^{2P} \left\langle \left(n_R^{\underline{S}[t]} \right)^2 - n_R^{\underline{S}[t]} n_{\bar{R}}^{\underline{S}[t]} \right\rangle_t + \sum_{R \neq R' \neq \bar{R}}^{2P} \left\langle a_R^{\mu[t]} a_{R'}^{\mu[t]} \right\rangle_t \left\langle n_R^{\underline{S}[t]} n_{R'}^{\underline{S}[t]} \right\rangle_t \\
&= \sum_{R=1}^{2P} \left\langle \left(n_R^{\underline{S}[t]} \right)^2 - n_R^{\underline{S}[t]} n_{\bar{R}}^{\underline{S}[t]} \right\rangle_t + \sum_{R \neq R' \neq \bar{R}}^{2P} \left(\frac{1}{P} \sum_{\mu=0}^{P-1} a_R^{\mu[t]} a_{R'}^{\mu[t]} \right) \left\langle n_R^{\underline{S}[t]} n_{R'}^{\underline{S}[t]} \right\rangle_t \\
&= \sum_{R=1}^{2P} \left\langle \left(n_R^{\underline{S}[t]} \right)^2 - n_R^{\underline{S}[t]} n_{\bar{R}}^{\underline{S}[t]} \right\rangle_t.
\end{aligned} \tag{6}$$

This sum over $2P$ terms can however be written as a sum over P terms,

$$\begin{aligned}
\sigma_\Omega^2 &= \sum_{R=1}^{2P} \left\langle \left(n_R^{S[t]} \right)^2 - n_R^{S[t]} n_{\bar{R}}^{S[t]} \right\rangle_t \\
&= \sum_{R=1}^P \left\langle \left(n_R^{S[t]} \right)^2 - n_R^{S[t]} n_{\bar{R}}^{S[t]} + \left(n_{\bar{R}}^{S[t]} \right)^2 - n_{\bar{R}}^{S[t]} n_R^{S[t]} \right\rangle_t \\
&= \sum_{R=1}^P \left\langle \left(n_R^{S[t]} \right)^2 - 2n_R^{S[t]} n_{\bar{R}}^{S[t]} + \left(n_{\bar{R}}^{S[t]} \right)^2 \right\rangle_t \\
&= \sum_{R=1}^P \left\langle \left(n_R^{S[t]} - n_{\bar{R}}^{S[t]} \right)^2 \right\rangle_t \equiv \left\langle \sum_{R=1}^P \left(n_R^{S[t]} - n_{\bar{R}}^{S[t]} \right)^2 \right\rangle_t.
\end{aligned} \tag{7}$$

All the above is for a given realization of the quenched disorder Ω . The ensemble-average is now performed over the various possible realizations of quenched disorder. The values of $n_R^{S[t]}$ and $n_{\bar{R}}^{S[t]}$ for each R will depend on the precise form of Ω .

The ensemble-average is denoted as $\langle \dots \rangle_\Omega$, and for simplicity the notation $\langle \sigma_\Omega^2 \rangle_\Omega = \sigma^2$ is defined. This ensemble-average is performed on either side of Equation 7,

$$\sigma^2 = \left\langle \left\langle \sum_{R=1}^P \left(n_R^{S[t]} - n_{\bar{R}}^{S[t]} \right)^2 \right\rangle_t \right\rangle_\Omega \tag{8}$$

yielding the volatility in the attendance $A(t)$. However as in Figure 2, the numerical simulations are typically performed for the volatility of the number of traders choosing option 1 (e.g. buy). Fortunately a simple relationship can be derived between the two as follows. Going back to the original definitions given for the attendance (Equation 1) and substituting into Equation 5, gives

$$\sigma^2 = \langle \langle [n_1(t) - n_0(t)]^2 \rangle_t \rangle_\Omega. \tag{9}$$

It is known that the total number of traders $N = n_1(t) + n_0(t)$, hence

$$\sigma^2 = \langle \langle [2n_1(t) - N]^2 \rangle_t \rangle_\Omega. \tag{10}$$

By the symmetry of the game however, it is expected that

$$\langle \langle [n_1(t)] \rangle_t \rangle_\Omega = \langle \langle [n_0(t)] \rangle_t \rangle_\Omega = \frac{N}{2} \tag{11}$$

and hence

$$\begin{aligned}
\sigma^2 &= \left\langle \left\langle \left[2n_1(t) - 2 \langle \langle [n_1(t)]^2 \rangle_t \rangle_\Omega \right]^2 \right\rangle_t \right\rangle_\Omega \\
&= 4 \left\langle \left\langle \left[n_1(t) - \langle \langle [n_1(t)]^2 \rangle_t \rangle_\Omega \right]^2 \right\rangle_t \right\rangle_\Omega \\
&= 4\sigma_1^2.
\end{aligned} \tag{12}$$

This leaves the result that the ensemble and time-averaged volatility of the number of agents choosing a given option is given by σ_1 , where

$$\sigma_1^2 = \frac{1}{4} \left\langle \left\langle \sum_{R=1}^P \left(n_R^{S[t]} - n_{\frac{S[t]}{R}} \right)^2 \right\rangle_t \right\rangle_{\Omega}. \quad (13)$$

Equation 13 is an important intermediary result for the Crowd-Anticrowd theory. Before proceeding to treat it analytically, it is important to evaluate it numerically to see how well it describes the numerical results of the Savit curve. If this is successful, we will have provided a proof-of-concept of the Crowd-Anticrowd approach. In particular, it will give us confidence that the Crowd-Anticrowd approach hasn't thrown out any of the essential physics so far, and reassure us that it is worth proceeding with an analytic evaluation of Equation 13.

Figure 7 confirms that the Crowd-Anticrowd theory of Equation 13 does indeed work. The solid curves represent the ensemble and time-averaged standard deviation of the number of agents choosing a given option, obtained by recording the number of agents choosing option 1 at every timestep. The dashed curves show the ensemble and time-averaged standard deviation calculated using Equation 13. (For the purpose of calculation, the numbers of agents using each R 'th ranked strategy were recorded at each timestep for 1000 turns of the game after initial transient effects had died down. The volatility for a run of the game was hence calculated over this time period. Finally an average was taken over 16 runs of the game to simulate the configuration averaging in Equation 13). As can be seen from Figure 7, the results show that Equation 13 captures the essential physics underlying the fluctuations in the Minority Game.

3.3 Quantitative theory

Equation 13 provides us with an exact theory for the time-averaged fluctuations in the MG. However some form of approximation must be introduced in order to reduce Equation 13 to an analytic expression. It turns out that Equation 13 can be manipulated in a variety of ways, depending on the level of approximation that one is prepared to make. The precise form of any resulting analytic expression will obviously depend on the details of the approximations made.

In this Section, we will approach the problem of evaluating Equation 13 analytically by first relabelling strategies. Specifically, the sum in Equation 13 is re-written to be over a *virtual-point ranking* K and not the decimal form R . Consider the variation in points for a given strategy, as a function of time for a given realization of the quenched disorder Ω . Figure 8 provides a schematic representation of how the scores of three such strategies, and their three anti-correlated strategies, might vary in time (particularly for lower m). The ranking (i.e. label) of a given strategy in terms of virtual-points score is changing all the time since the individual strategies have a variation in virtual-points which varies rapidly (see e.g. the black curve in Figure 8). This implies that the specific identity of the 'n'th highest-scoring strategy' is changing all the time. It also implies that $n_{\frac{S[t]}{R}}^{S[t]}$ is changing rapidly in time. In order to proceed, we shift the focus

onto the time-evolution of the highest-scoring strategy, second highest-scoring strategy etc. This has a much smoother time-evolution than the time-evolution for a given strategy $S_R[t]$. In short, *the focus is shifted from the time-evolution of the points of a given strategy (i.e. from $S_R[t]$) to the time-evolution of the points of the n 'th highest scoring strategy (i.e. to $S_K[t]$)*. From this point of view, Figure 8 should now be viewed in terms of virtual-point ranking K . Figure 9 is a schematic representation of how the scores of the two top scoring strategies from Figure 8 vary, using the new virtual-point ranking scheme. The label K is used to denote the rank in terms of strategy score, i.e. $K = 1$ is the highest scoring strategy position, $K = 2$ is the second highest-scoring strategy position etc. with

$$S_{K=1} > S_{K=2} > S_{K=3} > S_{K=4} > \dots \quad (14)$$

A given strategy, e.g. 0000, may at a given timestep have label $K = 1$, while a few timesteps later have label $K = 5$. Because it is known that $S_R = -S_{\bar{R}}$ (i.e. strategy scores start off all at zero), then we know that $S_K = -S_{\bar{K}}$. Equation 13 can hence be rewritten exactly as

$$\sigma_1^2 = \frac{1}{4} \left\langle \left\langle \sum_{K=1}^P \left(n_K^{S[t]} - n_{\bar{K}}^{S[t]} \right)^2 \right\rangle_t \right\rangle_{\Omega}. \quad (15)$$

Note that the quantities $n_K^{S[t]}$ and $n_{\bar{K}}^{S[t]}$ will fluctuate in time, but far less so than the individual strategy quantities $n_R^{S[t]}$ and $n_{\bar{R}}^{S[t]}$ in Equation 13. As can be seen from Figure 9 (e.g. black curve), the time-evolution of the strategy scores is such that the points for a given K tend to fluctuate around a mean value. It is now assumed that the spread in traders across the strategy space is fairly uniform, i.e. Ω is a fairly uniform matrix. This will be reasonable for small m , which is the focus of this analysis. Hence it is expected that the number of traders playing the strategy in position K at any timestep t , will also fluctuate around some mean value:

$$n_K^{S[t]} = n_K + \varepsilon_K(t), \quad (16)$$

where $\varepsilon_K(t)$ is assumed to be a white noise term with zero mean and small variance. Here n_K is the mean value. Hence,

$$\begin{aligned} \sigma_1^2 &= \frac{1}{4} \left\langle \sum_{K=1}^P \left\langle [n_K + \varepsilon_K(t) - n_{\bar{K}} - \varepsilon_{\bar{K}}(t)]^2 \right\rangle_t \right\rangle_{\Omega} \\ &= \frac{1}{4} \left\langle \sum_{K=1}^P \left\langle [(n_K - n_{\bar{K}}) + (\varepsilon_K(t) - \varepsilon_{\bar{K}}(t))]^2 \right\rangle_t \right\rangle_{\Omega} \\ &= \frac{1}{4} \left\langle \sum_{K=1}^P \left\langle [n_K - n_{\bar{K}}]^2 + [\varepsilon_K(t) - \varepsilon_{\bar{K}}(t)]^2 + [2(n_K - n_{\bar{K}})(\varepsilon_K(t) - \varepsilon_{\bar{K}}(t))] \right\rangle_t \right\rangle_{\Omega} \\ &\approx \frac{1}{4} \left\langle \sum_{K=1}^P \left\langle [n_K - n_{\bar{K}}]^2 \right\rangle_t \right\rangle_{\Omega} = \frac{1}{4} \left\langle \sum_{K=1}^P [n_K - n_{\bar{K}}]^2 \right\rangle_{\Omega}, \end{aligned} \quad (17)$$

since the latter two terms involving noise will average out to be small. The resulting expression involves no time dependence. The averaging over Ω

can then be taken inside the sum. The individual terms in the sum, i.e. $\langle [n_K - n_{\overline{K}}]^2 \rangle_\Omega$, are just an expectation value of a function of two variables n_K and $n_{\overline{K}}$. Each term can therefore be rewritten exactly using the joint probability distribution for n_K and $n_{\overline{K}}$, which we shall call $P(n_K, n_{\overline{K}})$. Hence,

$$\begin{aligned}\sigma_1^2 &= \frac{1}{4} \sum_{K=1}^P \langle [n_K - n_{\overline{K}}]^2 \rangle_\Omega \\ &= \frac{1}{4} \sum_{K=1}^P \sum_{n_K=0}^N \sum_{n_{\overline{K}}=0}^N [n_K - n_{\overline{K}}]^2 P(n_K, n_{\overline{K}}),\end{aligned}\tag{18}$$

where the standard probability result involving functions of two variables has been used. So how can we evaluate Equation 18? In general, it will depend on the detailed form of the joint probability function $P(n_K, n_{\overline{K}})$ which in turn will depend on the ensemble of quenched disorders $\{\Omega\}$ which are being averaged over.

We will start off by looking at Equation 18 in the limiting case where the averaging over the quenched disorder matrix is dominated by the matrices Ω which are nearly flat. This will be a good approximation for small m since in this limit the standard deviation of an element in Ω (i.e. the standard deviation in bin-size) is much smaller than the mean bin-size. In this limiting case, there are several nice features:

- in addition to the ranking in terms of virtual-points, i.e. $S_{K=1} > S_{K=2} > S_{K=3} > S_{K=4} > \dots$ (this holds by definition of the labels $\{K\}$), we will also have

$$n_{K=1} > n_{K=2} > n_{K=3} > n_{K=4} > \dots$$

[Note that the ordering in terms of the labels $\{R\}$ would not be sequential, i.e. it is *not* true that $n_{R=1} > n_{R=2} > n_{R=3} > n_{R=4} > \dots$] Hence the rankings in terms of highest virtual-points and popularity are identical.

- it is guaranteed that the strategy \overline{K} , which is anticorrelated to strategy K , occupies position $\overline{K} = 2P + 1 - K$ in this popularity-ranked list.
- the probability distribution $P(n_K, n_{\overline{K}})$ will be sharply peaked around the n_K and $n_{\overline{K}}$ values given by the expected values for a flat quenched-disorder matrix Ω . We will call these values \overline{n}_K and $\overline{n}_{\overline{K}}$.

The last point implies that $P(n_K, n_{\overline{K}}) \propto \delta(n_K - \overline{n}_K) \delta(n_{\overline{K}} - \overline{n}_{\overline{K}})$ and so

$$\sigma_1^2 = \frac{1}{4} \sum_{K=1}^P [\overline{n}_K - \overline{n}_{\overline{K}}]^2.\tag{19}$$

We note that there is a very simple interpretation of Equation 19. It represents the sum of the variances for each crowd-anticrowd pair. For a given strategy K there is an anticorrelated strategy \overline{K} . The n_K agents

using strategy K are doing the *opposite* to the $n_{\overline{K}}$ agents using strategy \overline{K} *irrespective* of the history bit-string. Hence the effective group-size for each crowd-anticrowd pair is $n_K^{eff} = \overline{n_K} - \overline{n_{\overline{K}}}$: this represents the net step-size d of the crowd-anticrowd pair in a random-walk contribution to the total variance. Hence, the net contribution by this crowd-anticrowd pair to the variance is given by

$$\begin{aligned} [\sigma_1^2]_{K\overline{K}} &= \frac{1}{4}[\sigma^2]_{K\overline{K}} = \frac{1}{4} \cdot 4pqd^2 = pqd^2 \\ &= \frac{[n_K^{eff}]^2}{4} = \frac{1}{4} [\overline{n_K} - \overline{n_{\overline{K}}}]^2. \end{aligned} \quad (20)$$

where $p = q = 1/2$ for a random walk. Since all the strong correlations have been removed (i.e. anti-correlations) it can be happily assumed that the separate crowd-anticrowd pairs execute random walks which are *uncorrelated* with respect to each other. [Recall the properties of the RSS - all the remaining strategies are uncorrelated]. Hence the total variance is given by the sum of the individual variances,

$$\sigma_1^2 = \sum_{K=1}^P [\sigma_1^2]_{K\overline{K}} = \frac{1}{4} \sum_{K=1}^P [\overline{n_K} - \overline{n_{\overline{K}}}]^2, \quad (21)$$

which corresponds exactly to Equation 19.

4 Limiting cases of Crowd-Anticrowd theory

4.1 Flat quenched disorder matrix Ω , low m

Explicit expressions for the case of a flat quenched disorder matrix Ω can now be calculated. In this limit each element of Ω has a mean of $N/(2P)^s$ agents per ‘bin’. For the case $s = 2$, the expected number of traders whose highest scoring strategy is the strategy occupying position K at timestep t , will therefore be given by summing the appropriate rows and columns of this quenched disorder matrix Ω . The matrix Ω is flat, so any re-ordering has no effect on the form of the matrix. Figure 10 provides a schematic representation of Ω with $m = 2$, $s = 2$, in the RSS. These strategies are now ranked according to the value of K . The shaded elements represent those agents which hold a strategy that is ranked 4th highest in score, i.e. $K = 4$. Any trader using the strategy in position $K = 4$ cannot have any strategy with a higher position, by definition of the rules of the game. (The traders use their highest scoring strategy). Hence the traders using the strategy in position $K = 4$ must lie in one of the shaded bins. Since it is assumed that the coverage of the bins is uniform, the expected number of agents using the strategy in position $K = 4$ is given by

$$\begin{aligned} \overline{n_{K=4}} &= N \cdot \frac{1}{(2P)^2} \sum (\text{shaded bins}) \\ &= N \cdot \frac{1}{64} \cdot [(8-3) + (8-3) - 1] \\ &= \frac{9}{64} N. \end{aligned} \quad (22)$$

For more general m and s values this becomes

$$\begin{aligned}
\overline{n_K} &= \frac{N}{(2P)^s} [s(2P-K)^{s-1} + \frac{s(s-1)}{2}(2P-K)^{s-2} + \dots + 1] \quad (23) \\
&= \frac{N}{(2P)^s} \sum_{r=0}^{s-1} \frac{s!}{(s-r)!r!} [2P-K]^r \\
&= \frac{N}{(2P)^s} ([2P-K+1]^s - [2P-K]^s) \\
&= N \cdot \left(\left[1 - \frac{(K-1)}{2P} \right]^s - \left[1 - \frac{K}{2P} \right]^s \right),
\end{aligned}$$

with $P \equiv 2^m$. In the case where each agent holds two strategies, $s = 2$, $\overline{n_K}$ can be simplified to

$$\begin{aligned}
\overline{n_K} &= N \cdot \left(\left[1 - \frac{(K-1)}{2P} \right]^2 - \left[1 - \frac{K}{2P} \right]^2 \right) \quad (24) \\
&= \frac{(2^{m+2} - 2K + 1)}{2^{2(m+1)}} N.
\end{aligned}$$

Similarly for $\overline{n_{\overline{K}}}$ the simplification is as follows:

$$\begin{aligned}
\overline{n_{\overline{K}}} &= \frac{(2^{m+2} - 2\overline{K} + 1)}{2^{2(m+1)}} N \quad (25) \\
&= \frac{(2K - 1)}{2^{2(m+1)}} N,
\end{aligned}$$

where the relation $\overline{K} = 2P - K + 1 \equiv 2^{m+1} - K + 1$ is used. It is emphasized that these results depend on the assumption that the averages are dominated by the effects of flat distributions for the quenched disorder matrix Ω , and hence will only be quantitatively valid for low m .

Using Equations 24 and 25 in Equation 19 gives

$$\begin{aligned}
\sigma_1^2 &= \frac{1}{4} \sum_{K=1}^P \left[\frac{(2^{m+2} - 2K + 1)}{2^{2(m+1)}} N - \frac{(2K - 1)}{2^{2(m+1)}} N \right]^2 \quad (26) \\
&= \frac{N^2}{2^{4(m+1)}} \sum_{K=1}^P [2^{m+1} - 2K + 1]^2 \\
&= \frac{N^2}{3 \cdot 2^{m+2}} (1 - 2^{-2(m+1)}),
\end{aligned}$$

and hence

$$\sigma_1^{\text{delta } f} = \frac{N}{\sqrt{3} \cdot 2^{\frac{m}{2}+1}} (1 - 2^{-2(m+1)})^{\frac{1}{2}}, \quad (27)$$

which is valid for small m . Numerical results show that this is indeed the case. (The rationale behind the choice of superscript will become apparent shortly.)

4.2 Non-flat quenched disorder Ω at low m

The appearance of a significant number of non-flat quenched disorder matrices Ω in the ensemble, implies that the standard deviation for each ‘bin’ is now significant, i.e. non-negligible compared to the mean. This will be increasingly true as m increases. In this case, the general analysis is much more complicated, and should really appeal to the dynamics. However, an approximate theory which gives good agreement with the numerical results can be developed. The features for the case of ensembles containing a significant number of non-flat quenched disorder matrices Ω are as follows:

- By definition of the labels $\{K\}$, the ranking in terms of virtual-points is retained, i.e. $S_{K=1} > S_{K=2} > S_{K=3} > S_{K=4} > \dots$ is always true. However, the disorder in the matrix Ω distorts the number of agents playing a given strategy away from the flat-matrix results. Hence it is not in general true that $n_{K=1} > n_{K=2} > n_{K=3} > n_{K=4} > \dots$, and hence the rankings in terms of highest virtual-points and popularity are no longer identical.
- Instead we have that $n_{K'} > n_{K''} > n_{K'''} > n_{K''''} > \dots$, where the label K' need not equal 1, and K'' need not equal 2 etc.. It is however possible to introduce a new label $\{Q\}$ which will rank the strategies in terms of popularity, i.e.

$$n_{Q=1} > n_{Q=2} > n_{Q=3} > n_{Q=4} > \dots,$$

where $Q = 1$ represents K' , $Q = 2$ represents K'' , etc.

With this in mind, we will return to the original general form for the volatility in Equation 18, but rewrite it slightly as follows:

$$\begin{aligned} \sigma_1^2 &= \frac{1}{4} \sum_{K=1}^P \sum_{n_K=0}^N \sum_{n_{\overline{K}}=0}^N [n_K - n_{\overline{K}}]^2 P(n_K, n_{\overline{K}}) \\ &= \frac{1}{8} \sum_{K=1}^{2P} \sum_{n_K=0}^N \sum_{n_{\overline{K}}=0}^N [n_K - n_{\overline{K}}]^2 P(n_K, n_{\overline{K}}) \\ &= \frac{1}{8} \sum_{K=1}^{2P} \sum_{K'=1}^{2P} \left\{ \sum_{n_K=0}^N \sum_{n_{K'}=0}^N [n_K - n_{K'}]^2 P(n_K, n_{K'}) \right\} f_{K', \overline{K}}, \end{aligned} \quad (28)$$

where the probability that $K' = \overline{K}$ is given by $f_{K', \overline{K}} = \delta_{K'=\overline{K}}$ and $\overline{K} = 2P + 1 - K$. So far, this manipulation is exact.

A switch is now made to the popularity-labels $\{Q\}$. Consider any particular strategy which was labelled previously by K and is now labelled by Q . Unlike the case of the flat disorder matrix, it is *not* guaranteed that this strategy’s anticorrelated partner will lie in position $\overline{Q} = 2P + 1 - Q$. This is because of the relabelling operation: all that can be said is that the strategy R has changed label from $K \rightarrow Q(K)$ while the anticorrelated strategy has changed label from $\overline{K} \rightarrow \overline{Q}(\overline{K})$ and that in general $\overline{Q} \neq 2P + 1 - Q$.

As a result of the relabelling, $n_{Q=1} > n_{Q=2} > n_{Q=3} > n_{Q=4} > \dots$ as stated earlier. Assuming that the main effect of the non-flat matrix was to shuffle these numbers, as opposed to altering their values, it can be assumed that as a zeroth-order approximation the values of $n_{Q=1}, n_{Q=2}, n_{Q=3}, \dots$ etc. are still sharply peaked around the expected values obtained for the flat-matrix case, i.e. it is assumed that the probability distribution $P(n_{Q(K)}, n_{Q'(\overline{K})})$ will be sharply peaked around the $n_{Q(K)}$ and $n_{Q'(\overline{K})}$ values given by the expected values for the (nearly flat) quenched-disorder matrix Ω . Lets call these values $\overline{n_Q}$ and $\overline{n_{Q'}}$ where the intrinsic dependence of Q on K has been dropped. Hence $P(n_Q, n_{Q'}) \propto \delta(n_Q - \overline{n_Q})\delta(n_{Q'} - \overline{n_{Q'}})$ with $\overline{n_Q}$ and $\overline{n_{Q'}}$ given by the box-counting method (see Figure 10 but with K, K' replaced by Q, Q'). The volatility becomes, after relabelling:

$$\sigma_1^2 = \frac{1}{8} \sum_{Q=1}^{2P} \sum_{Q'=1}^{2P} \left\{ \sum_{n_Q=0}^N \sum_{n_{Q'}=0}^N [n_Q - n_{Q'}]^2 P(n_Q, n_{Q'}) \right\} f_{Q', \overline{Q}}, \quad (29)$$

where $f_{Q', \overline{Q}}$ is the probability that strategy with label Q' is anticorrelated to \overline{Q} . Substituting in $P(n_Q, n_{Q'}) \propto \delta(n_Q - \overline{n_Q})\delta(n_{Q'} - \overline{n_{Q'}})$ gives

$$\sigma_1^2 = \frac{1}{8} \sum_{Q=1}^{2P} \sum_{Q'=1}^{2P} [\overline{n_Q} - \overline{n_{Q'}}]^2 f_{Q', \overline{Q}}, \quad (30)$$

where the function $f_{Q', \overline{Q}}$, which is the probability that the strategy with label Q' is the anticorrelated strategy \overline{Q} , still needs to be specified.

So what should the form of $f_{Q', \overline{Q}}$ be? In principle, it should include the effects of market impact/dynamical feedback which develops as the game progresses, in addition to the effects of the disorder. An exact expression for this term is yet to be found. However, two possibilities have been tried:

(i) assume a form that depends on m and N . This approach was first pursued in Ref. [16] and gives good analytic agreement with the numerical simulations (see later Figure 15). It will be discussed shortly.

(ii) assume that the probability that Q' is the anticorrelated strategy \overline{Q} , is given by $1/(2P)$ and is *independent* of the label Q' . In this sense this is the opposite limit to the delta-function case for flat disorder matrix. Instead of being a delta-function at $Q' = \overline{Q} = 2P + 1 - Q$, it is said that the anticorrelated strategy \overline{Q} could be anywhere in the list of $1 \dots 2P$ strategies.

Case (ii) is the first approach we will pursue here. In this limiting case of $1/(2P)$, one obtains

$$\sigma_1^{flat f} = \frac{N}{\sqrt{3.2}^{(m+3)/2}} (1 - 2^{-2(m+1)})^{\frac{1}{2}}. \quad (31)$$

Comparing this with Equation 27 it can be seen that

$$\sigma_1^{flat f} = \frac{1}{\sqrt{2}} \sigma_1^{delta f} \approx 0.7 \sigma_1^{delta f}. \quad (32)$$

for the case of $s = 2$. It should be noted that Equation 27 can be derived from Equation 30 by letting $f_{Q', \overline{Q}}$ take a δ -function distribution $\delta_{Q', 2^{m+1}+1-Q}$ peaked at $Q' = 2^{m+1} + 1 - Q$, hence the superscript in Equation 27.

4.3 Non-flat quenched disorder Ω at high m

For the limit of high m , the granular nature of the disorder becomes important. In other words, the standard deviation in the number of traders in a given bin is now similar to the mean value hence the fluctuations (which are limited to integer numbers) are important. Note that for large m , these integer numbers tend to be 0's and 1's for each box (Q, Q') . It almost looks like the problem of fermions in energy levels - double occupancy does not occur. In this limit of high m (by high m it is meant that the number of strategies is greater than $N.s$, i.e. $2 \cdot 2^m > N.s$) there will be N crowds each representing one strategy and one agent. In the limit that $f_{Q', \overline{Q}} = 1/(2P)$, the probability that a strategy Q representing one agent is matched with its anticorrelated strategy in position \overline{Q} also representing one agent, is given by $N/2P$. The probability that a strategy Q representing one agent is matched with its anticorrelated strategy in position \overline{Q} which represents a strategy that no agent is using, is given by $1 - N/2P$. Using Equation 30 then gives,

$$\begin{aligned} \sigma_1^2 &= \frac{1}{8} \sum_{Q=1}^{2P} \sum_{Q'=1}^{2P} [\overline{n_Q} - \overline{n_{Q'}}]^2 f_{Q', \overline{Q}} \\ &= \frac{1}{4} \sum_{Q=1}^N \left\{ [(\overline{n_Q} = 1) - (\overline{n_{Q'}} = 1)]^2 \frac{N}{2P} + [(\overline{n_Q} = 1) - (\overline{n_{Q'}} = 0)]^2 \frac{2P - N}{2P} \right\}, \end{aligned} \quad (33)$$

where the sum is now performed over the N strategies that each have one agent subscribed, and the second summation over Q' has been absorbed by the extra probabilistic factors. Simplifying this expression gives,

$$\begin{aligned} \sigma_1^{flat f, high m} &= \left(\frac{1}{4} \sum_{Q=1}^N [(\overline{n_Q} = 1) - (\overline{n_{Q'}} = 0)]^2 \frac{2P - N}{2P} \right)^{\frac{1}{2}} \\ &= \left(\frac{1}{4} N \cdot \frac{2P - N}{2P} \right)^{\frac{1}{2}} \\ &= \frac{\sqrt{N}}{2} \left(1 - \frac{N}{2^{m+1}} \right)^{\frac{1}{2}}, \end{aligned} \quad (34)$$

where $P \equiv 2^m$ has been used. It should be noted that $\sigma_1^{delta f}$, $\sigma_1^{flat f}$ and $\sigma_1^{flat f, high m}$, are only limits with regards to the way that the agents are distributed amongst the elements in the quenched disorder matrix Ω . They do not provide strict bounds on the actual standard deviation of the numbers of agents choosing a given option in the simulation.

Figure 2 shows (small circles) σ_1 as measured from the simulation for individual quenched disorder matrices Ω , as a function of agent memory size m . The spread in values from individual runs, for a given m , indicates the extent to which the choice of Ω alters the dynamics of the MG.

The upper line at low m , is Equation 27 showing $\sigma_1^{\text{delta } f}$. The lower line at low m , is Equation 31 showing $\sigma_1^{\text{flat } f}$. The line at high m is Equation 34 showing $\sigma_1^{\text{flat } f, \text{high } m}$. Figure 11 shows $\sigma_1^{\text{delta } f}$, $\sigma_1^{\text{flat } f}$ and $\sigma_1^{\text{flat } f, \text{high } m}$, as a function of m for $s = 2, 4$ and 8 . Comparing the analytic curves with the numerical results seen in Figure 11, it can be seen that these analytic expressions capture the essential physics driving the variation in behaviour of the volatility. They have been obtained within a static framework, confirming that the volatility does not depend in a sensitive way on the details of the dynamics.

4.4 An investigation of strategy rankings

We now investigate more carefully a possible analytic form for $f_{Q', \overline{Q}}$. Recall Equation 30,

$$\sigma_1^2 = \frac{1}{8} \sum_{Q=1}^{2P} \sum_{Q'=1}^{2P} [\overline{n_Q} - \overline{n_{Q'}}]^2 f_{Q', \overline{Q}} \quad (35)$$

The probability distribution $f_{Q', \overline{Q}}$ gives the probability that the Q' 'th most popular strategy is the anticorrelated strategy to the Q 'th most popular strategy. It has already been stated that an exact form for $f_{Q', \overline{Q}}$ has yet to be found.

Figure 12 compares the theoretical values of n_Q calculated using Equation 23 for $s = 2$ and $N = 101$ (dashed lines) to numerical values taken from the MG simulation (solid lines). We have dropped the bar over n_Q for simplicity, since we are always talking about time-averages. The agreement is good. In this comparison it is necessary to consider the granular nature of the MG: this effect becomes increasingly important as the agents' memory size m increases. As such, the quantities n_Q are rounded to the nearest integer to account for the fact that agents exist only as integer values. This is subject to the constraint that

$$\sum_{Q=1}^{Q=2P} n_Q = N. \quad (36)$$

Only a limited number (call this B) terms should be included in this sum, subject to the condition that the partial sum equals N *after* the quantities n_Q have been rounded to the nearest integer. In addition any n_Q 's which are less than one, are rounded up to one if $Q \leq B$ such that the first B terms are all non-zero and sum to N . There are hence only B different strategies in play; note that $B \leq 2.2^m$ and $B \leq N$. Figure 13 shows $f_{Q', \overline{Q}}$ for $Q = 1$ as a function of Q' , taken from the numerical MG simulation at $m = 2, 5$ and 10 . We note the following properties:

- For small m ($m = 2$) the anticorrelated strategy to the most popular strategy (i.e. $Q = 1$) is at $Q' = 2^{m+1}$, i.e. it is the least popular strategy. Hence $f_{Q', \overline{Q}}$ resembles the δ -function limiting case mentioned above. Very few agents will therefore pick this anticorrelated strategy. Hence the crowd-anticrowd cancellation will be small and σ_1 will be large, as can be seen in Figures 11 and 2.

- As m increases ($m = 5$) a remarkable effect occurs: the peak in $f_{Q',\overline{Q}}$ moves up toward $Q' = 1$. Hence both $Q = 1$ and its anticorrelated partner \overline{Q} are now very popular. Whereas for $m = 2$ it seemed like there was an effective ‘repulsion’ between Q and \overline{Q} , for $m = 5$ this now seems more like an attraction. Amusingly, the shape of $f_{Q',\overline{Q}}$ for $m = 5$ is now reminiscent of the screening effect of a negative charge cloud around a positive charge placed at $Q = 1$, or even a bound electron-hole pair (i.e. exciton) with the crowd (anticrowd) playing the role of the positive (negative) charge. The consequence of this attraction which appears as m increases, is that the crowd and anticrowd become comparable in size, yielding a significant cancellation and hence small volatility as observed in the Savit curve (i.e. Figure 2).
- For large m ($m = 10$), the ability of the anticrowd to ‘screen’ the crowd has decreased yielding a rather flat distribution as shown.

Hence σ_1 is small for $m \sim 5-6$, in agreement with Figure 2. Note that, at intermediate m , the MG cannot fully ‘optimize’ itself by building crowds and anticrowds of exactly equal size. This is due to the initial quenched disorder Ω , and the random processes used to resolve the decisions of agents in the instances when they have strategies with equal past performance. This explains why the volatility does not go to zero at finite m , and why the label of ‘phase transition’ to separate the small and large m regimes in the Savit curve, is not strictly correct.

Figure 14 shows the spread of numerical values for different runs of the MG compared to the crowd-anticrowd theoretical calculation (solid circles) using Equation 30. In contrast to the previous theoretical curves which used analytic expressions for the probability function $f_{Q',\overline{Q}}$, the results for each m in Figure 14 have been obtained by generating the corresponding $f_{Q',\overline{Q}}$ numerically, as in Figure 13. The agreement is very good. The theoretical points tend to lie toward the high end of the numerical spread, for example at $m = 2$; this can be attributed to the fact that the theory neglects accidental degeneracies in the virtual-point ordered list $\{n_K\}$. It has been checked that including a stochastic (i.e. coin-toss) process to break such ties, reduces the theoretical σ values down toward the mid-point of the numerical spread.

4.5 Using approximate strategy rankings

We now return to a discussion of case (i) which was referred to earlier, and used in Ref. [16]. It turns out to be convenient to start with Equation 19 for the squared volatility of the number of agents choosing a given option,

$$\sigma_1^2 = \frac{1}{4} \sum_{K=1}^P [\overline{n_K} - \overline{\overline{n_K}}]^2. \quad (37)$$

It has been established that $S_{K=1} > S_{K=2} > S_{K=3} > S_{K=4} > \dots$ is always true and that for a flat quenched disorder matrix Ω a similar statement can be made for the numbers of agents using the K ’th ranked

scoring strategy, i.e. $n_{K=1} > n_{K=2} > n_{K=2} > n_{K=2} > \dots$. It is also guaranteed that the strategy \bar{K} , which is anticorrelated to strategy K , occupies position $\bar{K} = 2P + 1 - K$ in this performance-ranked list. Whilst assuming a flat quenched disorder matrix Ω is valid at low m , it is not however valid at high m . This is due to granular effects as the value of m is increased. It remains true that the strategy \bar{K} , which is anticorrelated to strategy K , occupies position $\bar{K} = 2P + 1 - K$ in the performance-ranked list, however there is no guarantee that the strategy represented by \bar{K} is even present in the game. It is possible, and indeed highly likely at high m , that the strategy \bar{K} was not picked by any of the agents at the start of the game. For example if $m = 8$, there are 512 strategies in the RSS, and for $N = 101$ and $s = 2$ there will only be up to 2×101 of the 512 possible strategies actually present in the game (repetition during initial strategy-picking is allowed).

To describe this situation, Ref. [16] introduced a probability $P(\bar{K} \in \mathcal{G})$. (We referred to this as case (i) earlier in the present paper). This corresponds to the following probability: given that strategy K is used, then $P(\bar{K} \in \mathcal{G})$ is the probability that strategy \bar{K} is a member of the set of strategies \mathcal{G} that have been chosen by the agents at the start of the game. Equation 19 is rewritten to include this probability:

$$\sigma_1^2 = \frac{1}{4} \sum_{K=1}^P [\bar{n}_K - P(\bar{K} \in \mathcal{G})\bar{n}_{\bar{K}}]^2 + \frac{1}{4} \sum_{K=1}^P [(1 - P(\bar{K} \in \mathcal{G}))\bar{n}_{\bar{K}}]^2. \quad (38)$$

The second term in Equation 38 accounts for those strategies which are not anti-correlated to any other strategy. We now recall Equation 23 which gives the mean number of agents when assuming a flat quenched disorder matrix Ω :

$$\bar{n}_K = N \left(\left[1 - \frac{(K-1)}{2P} \right]^s - \left[1 - \frac{K}{2P} \right]^s \right) \quad (39)$$

Taking into account the granular nature of the game, implies that the condition $\sum_{K=1}^{K=2P} \bar{n}_K = N$ should also be imposed. Hence only G terms in this sum should be included, subject to the condition that the partial sum equals N *after* the quantities \bar{n}_K have been rounded to the nearest integer. In addition, any \bar{n}_K 's which are less than one, are rounded up to one if $K \leq G$ such that the first G terms are all non-zero. There are hence only G different strategies in play; note that $G \leq 2 \cdot 2^m$ and $G \leq N$. The probability $P(\bar{K} \in \mathcal{G})$ is now the probability that the $[G+1-K]$ -th strategy is anticorrelated to the K -th strategy and is a member of the set \mathcal{G} of strategies chosen by agents at the start of the game. The variance can hence be written analytically as

$$\begin{aligned} \sigma_{an}^2 &= \frac{1}{4} \sum_{K=1}^{\frac{1}{2}(G-g)} [\bar{n}_K - P(\bar{K} \in \mathcal{G})\bar{n}_{G+1-K}]^2 \\ &\quad + \frac{1}{4} \sum_{K=1}^{\frac{1}{2}(G-g)} [(1 - P(\bar{K} \in \mathcal{G}))\bar{n}_{G+1-K}]^2 + \frac{g}{4} [n_{\frac{G+1}{2}}]^2, \end{aligned} \quad (40)$$

where $g = 0$ if G is even and $g = 1$ if G is odd. The first term represents the net effect after pairing off the agents playing anticorrelated strategies.

The second term in Equation 40 reintroduces those agents using strategies that were assumed to be anticorrelated to some more successful strategy, and hence were discarded unnecessarily in the first term. The third term in Equation 40 is due to the volatility of the group which remains unpaired in the case where the number of different strategies used in the calculation is odd. The third term is usually negligible compared to the first two. $P(\overline{K} \in \mathcal{G})$ can be approximated by $P(\overline{K} \in \mathcal{G}) = p$ for $p < 1$ and $P(\overline{K} \in \mathcal{G}) = 1$ for $p > 1$, where $p = N/(2.2^m)$. Although the form for $P(\overline{K} \in \mathcal{G})$ can be made more accurate, the present expression is reasonable since there are only of order N strategies out of a possible maximum of 2.2^m which can actually be in play at any one time. Hence, as expected, $P(\overline{K} \in \mathcal{G})$ is zero when $N \ll 2.2^m$ and unity when $N \gg 2.2^m$. It has been checked that the analytic results for the volatility are fairly insensitive to the precise form of $P(\overline{K} \in \mathcal{G})$ as long as $P(\overline{K} \in \mathcal{G})$ satisfies the above expectations.

Figure 15 shows the full analytical expression for the volatility curves (solid lines) of the number of agents choosing a given option for $s = 2$, $s = 4$ and $s = 6$ with $N = 101$, compared with the numerical simulations (dashed line). Note that since m is integer, the curves are not smooth. The agreement between the analytic and numerical results is good across a wide range of m and s values. In particular, the analytic results capture the deepening of the minimum in the volatility as s decreases.

To summarize, both approaches (case (i) and case (ii)) are approximations to the exact theory of Equation 13. While the approximations adopted have some subtle differences of emphasis, the resulting expressions have in both cases captured the essential physics underlying the volatility, over a wide range of m and s values: the essence of this physics is the correlations in strategy space and the associated crowd-anticrowd behavior.

4.6 Reduced vs. Full Strategy Space

The volatility of the MG is qualitatively the same when played in both the FSS and the RSS [4]. Quantitatively the volatility of the MG when played using the RSS is very slightly larger than that of a game played using the FSS. One may therefore ask why the MG is so similar in characteristics when played in the RSS and the FSS, and hence why the crowd-anticrowd theory also provides a valid description for the MG when played in the FSS.

For a game played in the FSS there are $2^{2^m}/2.2^m$ distinct subsets of strategies. Each subset can be considered as a separate RSS. Note that the strategies that belong to a given RSS are optimally spread out across the corresponding FSS hypercube. Figure 3 shows the distribution of the 16, $m = 2$ strategies across the 4 dimensional hypercube. The positions of the strategies belonging to the RSS are such that no two strategies have a Hamming separation less than $2^m/2$. The same can be said for any other choice of RSS. Due to the nature of a RSS, then given similar strings of past outcomes from which to score strategies over, each strategy within the RSS attains a score in an uncorrelated or anticorrelated manner to any other strategy in the subset. Any other RSS within the FSS will score its strategies in a similar way, although slightly ‘out of phase’. For

example for $m = 3$, the first RSS to be considered could contain the strategy 00001111, and the second RSS considered could contain the strategy 01001111. It is easy to see that on 7 out of 8 occasions these two strategies would score in the same way. So, given the nature of the MG (i.e. over a sufficient period of time in a typical game, any history is just as likely to be followed by a ‘0’ or a ‘1’ for low m , whilst at high m cooperative effects die off), it can be seen that these two strategies from two separate RSS follow each other during a typical run of the game. This argument extends across all strategies in all of the $2^{2^m}/2.2^m$ distinct RSS’s within the FSS. Hence a game using the FSS behaves as if there are 2.2^m clusters of strategies and so is similar to a game played in the RSS. These clusters form the crowds and anticrowds of the theory and this clustering allows the use of just one RSS in the analysis of the MG.

We note that the present crowd-anticrowd theory, even within its RSS formulation, also provides a quantitative theory [20] to explain the surprising suppression of volatility observed numerically for the ‘Thermal Minority Game’ (TMG) [30]. In the TMG agents choose between their strategies using an exponential probability weighting. This reduction in σ for stochastic strategies seems fairly general: for example, the earlier work of Ref. [26] provided a modified MG in which agents with stochastic strategies also generate a smaller-than-random σ . We have shown [20] that incorporating stochastic strategy-use tends to increase the crowd-anticrowd cancellation thereby reducing σ below the random coin-toss limit. In addition we have shown [21] how the theory also works for a mixed population of such ‘thermal’ agents and non-thermal agents (i.e. $T = 0$). We refer to Refs. [20] and [21] for a detailed discussion and graphs showing the good quantitative agreement between the Crowd-Anticrowd theory and the numerical results.

To our knowledge, there is no other analytic theory which can match the range of quantitative agreement for these models. This suggests the Crowd-Anticrowd theory is an important milestone in such multi-agent systems, and possibly even Complex Systems in general. It is also pleasing from the point of view of physics methodology, since the basic underlying philosophy of accountly correctly for ‘inter-strategy’ correlations is already known to be successful in more conventional areas of many-body physics. This raises the interesting possibility that conventional many-body physics might be open to re-interpretation in terms of an appropriate multi-particle ‘game’: we leave this for future work.

5 Conclusion

We have given an in-depth presentation of the Crowd-Anticrowd theory in order to understand the time-averaged and configuration-averaged fluctuations in the MG system. The quantitative success of the Crowd-Anticrowd theory means that much of the time-averaged and ensemble-averaged properties of such MG-like systems can be understood without having to solve the detailed game dynamics. Since the theory depends on structure in strategy space, as opposed to the minority character of the game, we believe that the Crowd-Anticrowd theory will have applicability

for more general multi-agent systems. In particular, we are currently investigating the modifications that need to be made to the theory when the game is placed on a network, or there is some form of local connectivity between some (or all) agents. These findings will be reported elsewhere.

We believe that the Crowd-Anticrowd concept might serve as a fundamental theoretical concept for more general Complex Systems which mimic competitive multi-agent games. Obviously there will be some properties of MG games which cannot be described using such time- and configuration-averaged theories as used here. In particular, any observation of a real-world Complex System which is thought to resemble a multi-agent game, will more likely to correspond to a *single* run which evolves from a specific initial configuration of agents' strategies. This implies a particular Ω , hence the time-averagings within the Crowd-Anticrowd theory must be carried out for that particular choice of Ω [33]. We refer to Refs. [23, 24] for a detailed discussion of such run-specific dynamics. For time-dependent properties of a more general system, a dynamical form of the crowd-anticrowd approach can be developed in which the time-dependence of the crowd-anticrowd sizes is included specifically.

Acknowledgements Much of this work has benefited from our on-going research collaboration with Paul Jefferies and Pak Ming Hui.

References

- [1] D. Challet and Y.C. Zhang, Physica A **246**, 407 (1997).
- [2] B. Arthur, Amer. Econ. Rev. **84**, 406 (1994); Science **284**, 107 (1999).
- [3] N.F. Johnson, S. Jarvis, R. Jonson, P.Cheung, Y. Kwong and P.M. Hui, Physica A **258**, 230 (1998).
- [4] D. Challet and Y.C. Zhang, Physica A **256**, 514 (1998).
- [5] M. Marsili and D. Challet, Phys. Rev. E **64**, 056138 (2001).
- [6] D. Challet and M. Marsili, Phys. Rev. E **60**, 6271 (1999).
- [7] D. Challet, M. Marsili and R. Zecchina, Phys. Rev. Lett. **82**, 2203 (1999).
- [8] D. Challet, M. Marsili and Y.C. Zhang, Physica A **294**, 514 (2001).
- [9] M. Marsili and D. Challet, Adv. Complex Systems **1**, 1 (2000).
- [10] M. Marsili, D. Challet and R. Zecchina, Physica A **280**, 522 (2000).
- [11] D. Challet and M. Marsili, Phys. Rev. E **62**, 1862 (2000).
- [12] D. Challet, M. Marsili and R. Zecchina, Phys. Rev. Lett. **85**, 5008 (2000).
- [13] R. Savit, R. Manuca and R. Riolo, Phys. Rev. Lett. **82**, 2203 (1999). Interestingly, we had found a similarly shaped curve for the volatility in the El Farol problem (see Ref. [3]).
- [14] Y. Li, R. Riolo and R. Savit, Physica A **276**, 234 (2000).
- [15] Y. Li and R. Riolo and R. Savit, Physica A **276**, 265 (2000).
- [16] N.F. Johnson, M. Hart and P.M. Hui, Physica A **269**, 1 (1999).
- [17] M. Hart, P. Jefferies, N.F. Johnson and P.M. Hui, Physica A **298**, 537 (2001).
- [18] N.F. Johnson, P.M. Hui, Dafang Zheng, and M. Hart, J. Phys. A: Math. Gen. **32**, L427 (1999).
- [19] N.F. Johnson, M. Hart, P.M. Hui and D. Zheng, Int. J. of Th. and Applied Fin **3**, 443 (2000);
- [20] M.L. Hart, P. Jefferies, N.F. Johnson and P.M. Hui, Phys. Rev. E **63**, 017102 (2001).
- [21] P. Jefferies, M. Hart, N.F. Johnson, and P.M. Hui, J. Phys. A: Math. Gen. **33**, L409 (2000).
- [22] P. Jefferies, M.L. Hart, P.M. Hui, and N.F. Johnson, Eur. Phys. J. B **20**, 493 (2000); N.F. Johnson, D. Lamper, P. Jefferies, M.L. Hart and S. Howison, Physica A **298**, 222 (2001). The GCMG model was presented at the APFA1 conference in Dublin (1999) and at the first International Workshop of Applications of Statistical Physics to Financial Analysis in Palermo (September 1998).
- [23] M.L. Hart, P. Jefferies and N.F. Johnson, Physica A **311**, 275 (2002).
- [24] M.L. Hart, D. Lamper and N.F. Johnson, Physica A **316**, 649 (2002).

- [25] P. Jefferies, M.L. Hart and N.F. Johnson, Phys. Rev. E **65**, 016105 (2002).
- [26] N.F. Johnson, P.M. Hui, R. Jonson and T.S. Lo, Phys. Rev. Lett. **82**, 3360 (1999).
- [27] J.A.F. Heimeel and A.C.C. Coolen, Phys. Rev. E. **63**, 056121 (2001).
- [28] J.A.F. Heimeel, A.C.C. Coolen and D. Sherrington, Phys. Rev. E **65**, 016126 (2001).
- [29] A. Cavagna, Phys. Rev. E **59**, 3783 (1999).
- [30] A. Cavagna, J.P. Garrahan, I. Giardina and D. Sherrington, Phys. Rev. Lett. **83**, 4429 (1999); A. Cavagna, J.P. Garrahan, I. Giardina and D. Sherrington, Phys. Rev. Lett **85**, 5009 (2000).
- [31] J.P. Garrahan, E. Moro and D. Sherrington, Quant. Finance **1** 246 (2001).
- [32] See <http://www.unifr.ch/econophysics/minority>
- [33] Note that a single Ω ‘macrostate’ can still correspond to many possible ‘microstates’ for partitions of strategy allocation among the agents. Hence the Crowd-Anticrowd theory retained at the level of a given specified Ω , will still be of use for all games whose initial strategy allocations correspond to that same Ω .

FIGURE CAPTIONS

FIGURE 1 Minority Game (MG): at timestep t , each agent decides whether to enter a game where the choices are option 1 and option 0. A total of $n_0(t)$ agents choose 0 while $n_1(t)$ choose 1, with $n_0(t) + n_1(t) = N$.

FIGURE 2 Volatility (small circles) as measured from individual runs of numerical simulations, as a function of agent memory size m . Each run corresponds to a randomly-chosen quenched disorder matrix Ω . Upper line at low m is Equation 27 showing $\sigma_1^{delta f}$. Lower line at low m , is Equation 31 showing $\sigma_1^{flat f}$. Line at high m is Equation 34 showing $\sigma_1^{flat f, high m}$. Dashed line is random coin-toss limit.

FIGURE 3 An $m = 2$ strategy space together with some example strategies (left). The strategy space shown is known as the ‘Full Strategy Space’, FSS, and contains all possible permutations of the binary options 0 and 1 for each history. There are 2^{2^m} strategies in this space. The 2^m dimensional hypercube (right) shows all 2^{2^m} strategies from the full strategy space at its vertices.

FIGURE 4 Examples of the de Bruijn graph for $m = 1, 2$, and 3 . The probability that the outcome at time $t + 1$ will be a 1 (or 0) depends on the state at time t .

FIGURE 5 Example distribution for the tensor Ω describing the strategy allocation for $N = 101$ agents in the case of $m = 2$, and $s = 2$ in the reduced strategy space RSS.

FIGURE 6 Qualitative explanation of the competition between crowd-anticrowd sizes as a function of m . The group of agents whose highest strategy is R , provides a crowd since they will all use the same strategy at a particular time-step (and hence act in the same way regardless of the particular history bit-string at that timestep). Upper panel: run-averaged version of Figure 2, showing the run-averaged volatility of the number of agents choosing a particular option as a function of the memory size m .

FIGURE 7. Proof-of-concept of Crowd-Anticrowd approach. Graph shows volatility for the Minority Game as a function of memory size m , for $s = 2, 3, 4$ strategies per agent, and $N = 101$ agents. Solid curve: numerical simulation. Dashed curve: Crowd-Anticrowd theory, evaluated numerically using Equation 13. Random (coin-toss) limit $\sigma = \sqrt{N}/2 = 5.0$ is indicated.

FIGURE 8 Schematic representation of how the scores of three strategies and their three anti-correlated partners, might vary in time.

FIGURE 9 Same as Figure 8, but with strategies now ranked in terms of virtual-point ranking K . Hence shows the variation of the scores of the two top scoring strategies from Figure 8.

FIGURE 10 Schematic representation of Ω with $m = 2$, $s = 2$, in the RSS. The strategies are ranked according to the value of K . The shaded elements represent those agents whom hold a strategy that is ranked 4th

highest in score, i.e. $K = 4$.

FIGURE 11 Analytic forms of volatilities $\sigma_1^{delta f}$, $\sigma_1^{flat f}$ and $\sigma_1^{flat f, high m}$, as a function of m for $s = 2, 4$ and 8 . Also shown are the numerical values obtained from different simulation runs (triangles, crosses and circles). The results for $s = 2$ are the same as Figure 2.

FIGURE 12 Comparison between the theoretical values of n_Q calculated using Equation 23 for $s = 2$ and $N = 101$ (dashed lines) and the numerical values taken from the MG simulation (solid lines).

FIGURE 13 Form of $f_{Q', \overline{Q}}$ for $Q = 1$ as a function of Q' , taken from the numerical MG simulation at $m = 2, 5$ and 10 .

FIGURE 14 Volatility as a function of memory m for $s = 2$ and $N = 101$. The spread of numerical values for different runs of the MG (open circles) is compared to the Crowd-Anticrowd theoretical calculation using Equation 30 with numerically obtained values of $f_{Q', \overline{Q}}$ (solid circles).

FIGURE 15 Analytic theory for the volatility curves (solid lines: see Section 4.3) for $s = 2$, $s = 4$ and $s = 6$ with $N = 101$. Numerical simulations (dashed line) also shown, averaged over a limited number of runs (hence the jaggedness).

Figure 1

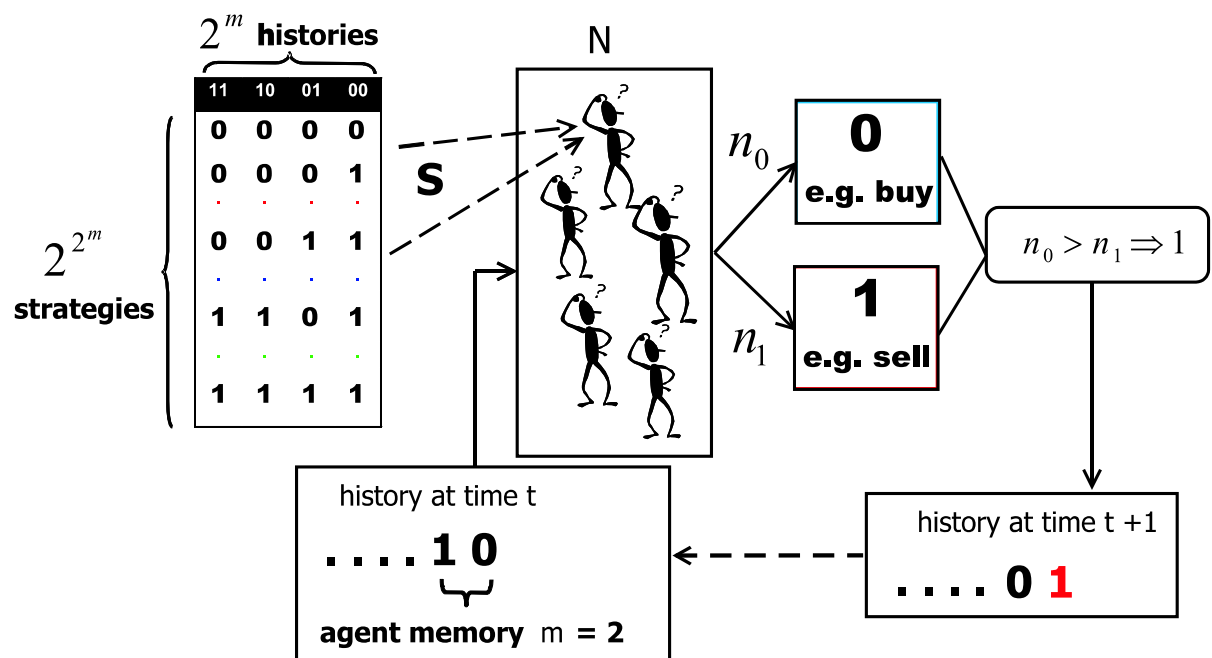


Figure 2

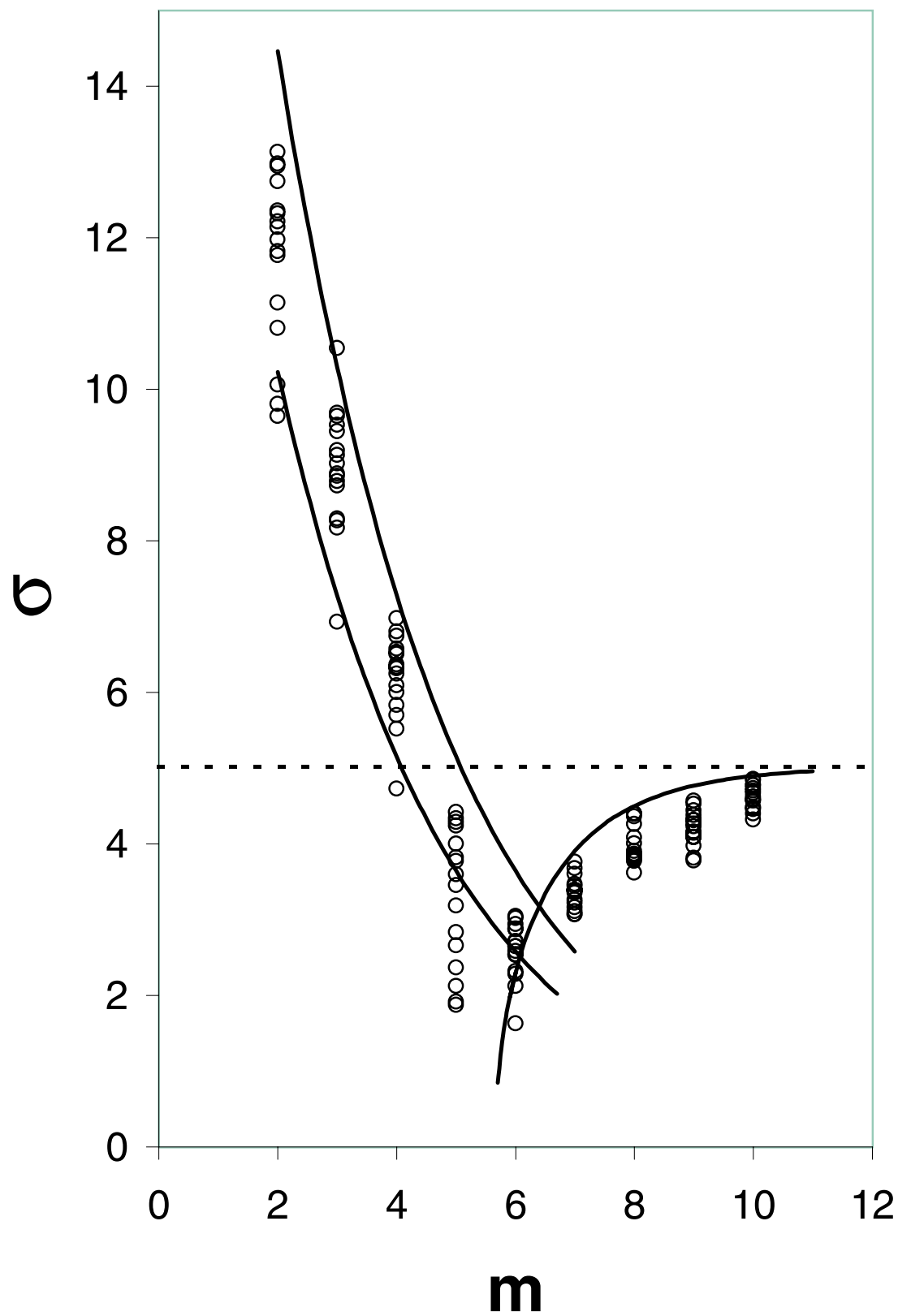
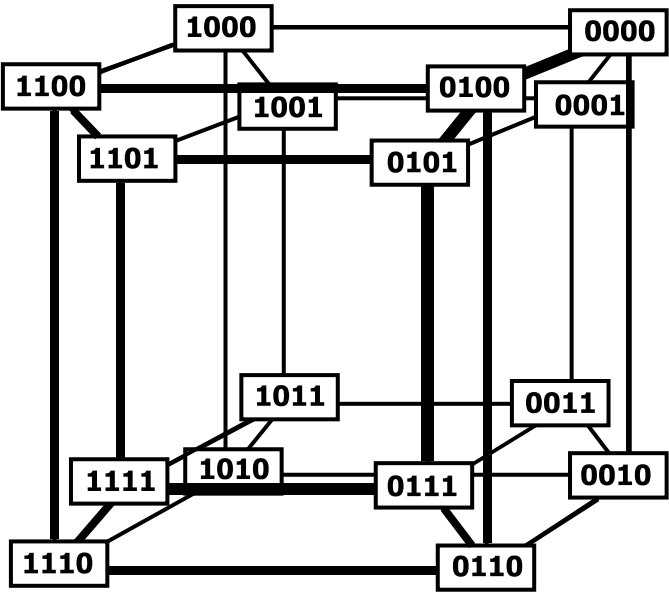


Figure 3

2^{2^m}

2^m histories			
11	10	01	00
0	0	0	0
0	0	0	1
.	.	.	.
0	0	1	1
.	.	.	.
0	1	1	1
.	.	.	.
1	1	1	1



$2^m=4$ dimensional hypercube

Figure 4

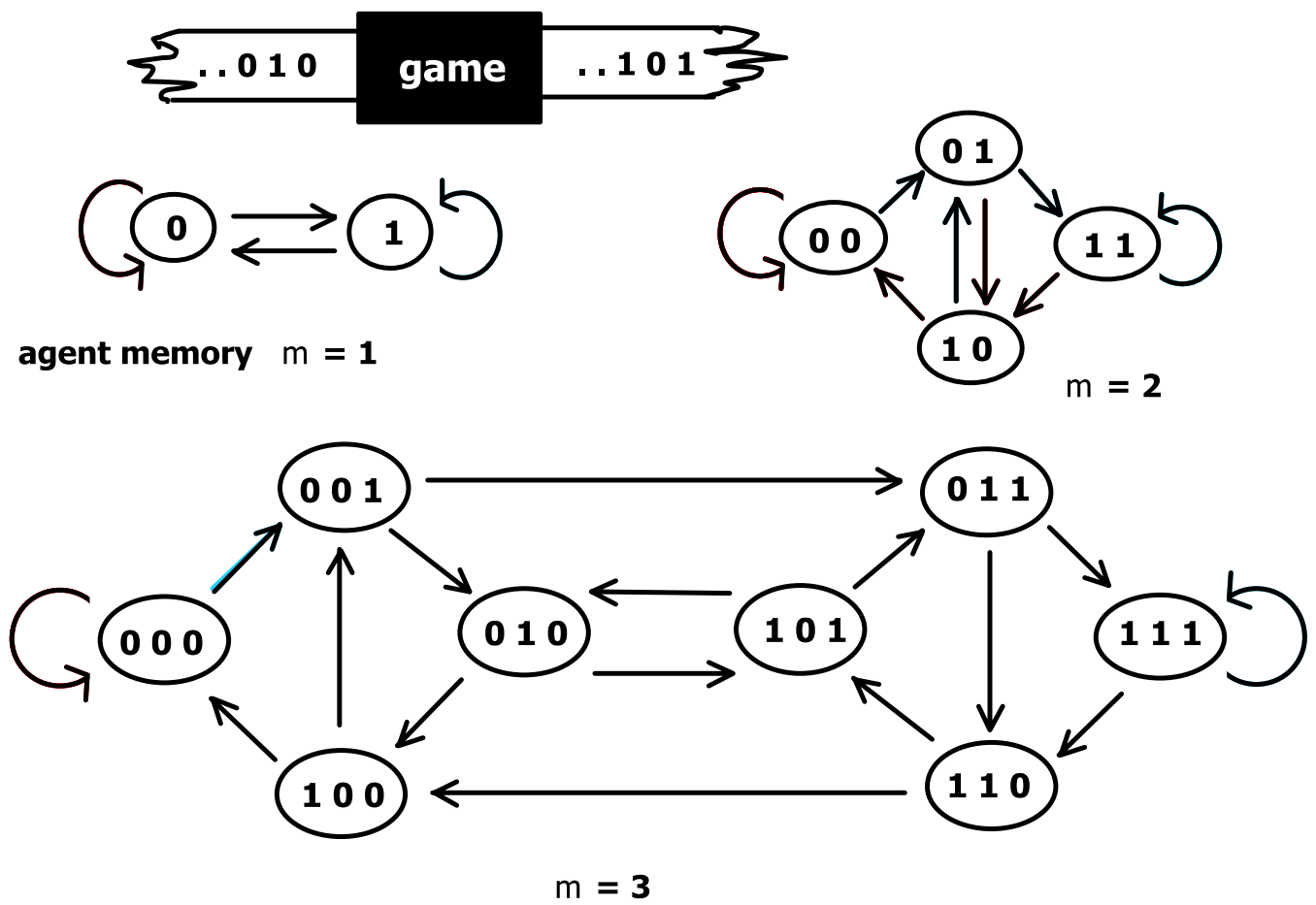
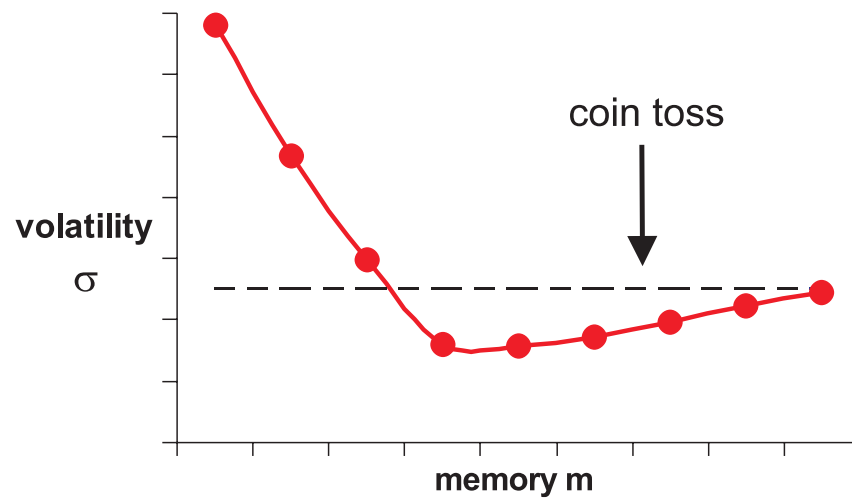


Figure 5

strategy R →

		1	2	3	4	5	6	7	8
Strategy R' ↓	1	1	2	1	0	1	1	1	1
	2	0	0	2	2	2	0	2	0
	3	2	1	0	3	1	0	2	1
	4	2	2	0	3	3	2	2	2
	5	1	1	0	2	3	3	2	0
	6	2	3	2	0	1	5	1	1
	7	0	1	4	7	2	1	0	0
	8	3	2	2	0	2	2	2	4

Figure 6



Regime	$2^{m+1} \ll N.s$	$2^{m+1} \sim N.s$	$2^{m+1} \gg N.s$
Crowd size	large	medium	~ 1
Anticrowd size	small	medium	~ 0
Net (<i>crowd</i> - <i>anticrowd</i>) pair size	large $\gg 1$	small	small ~ 1
# crowd - anticrowd pairs	$\sim 2^m \ll N$	$\sim 2^m < N$	$< 2^m \sim N$

Figure 7

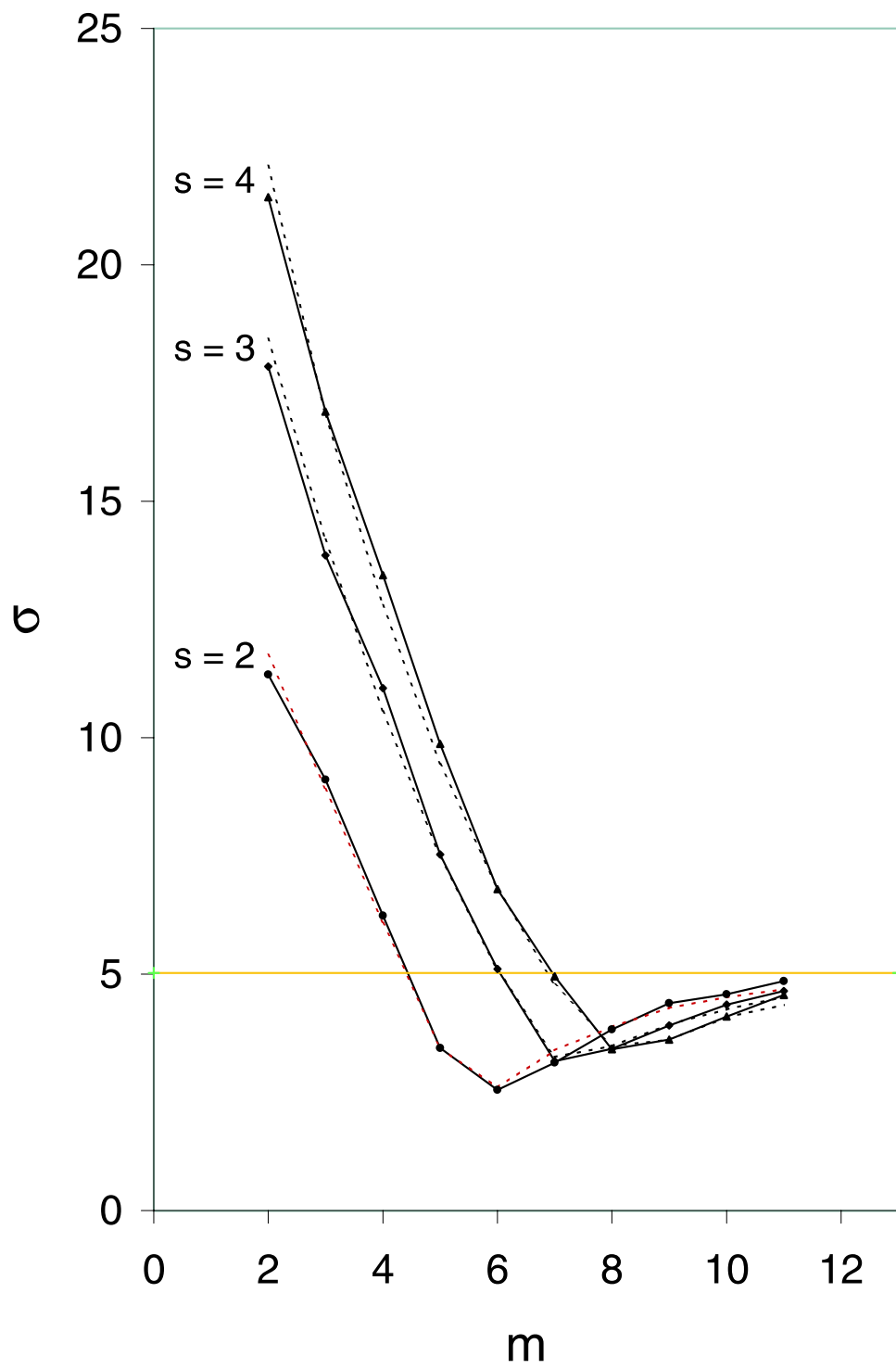


Figure 8

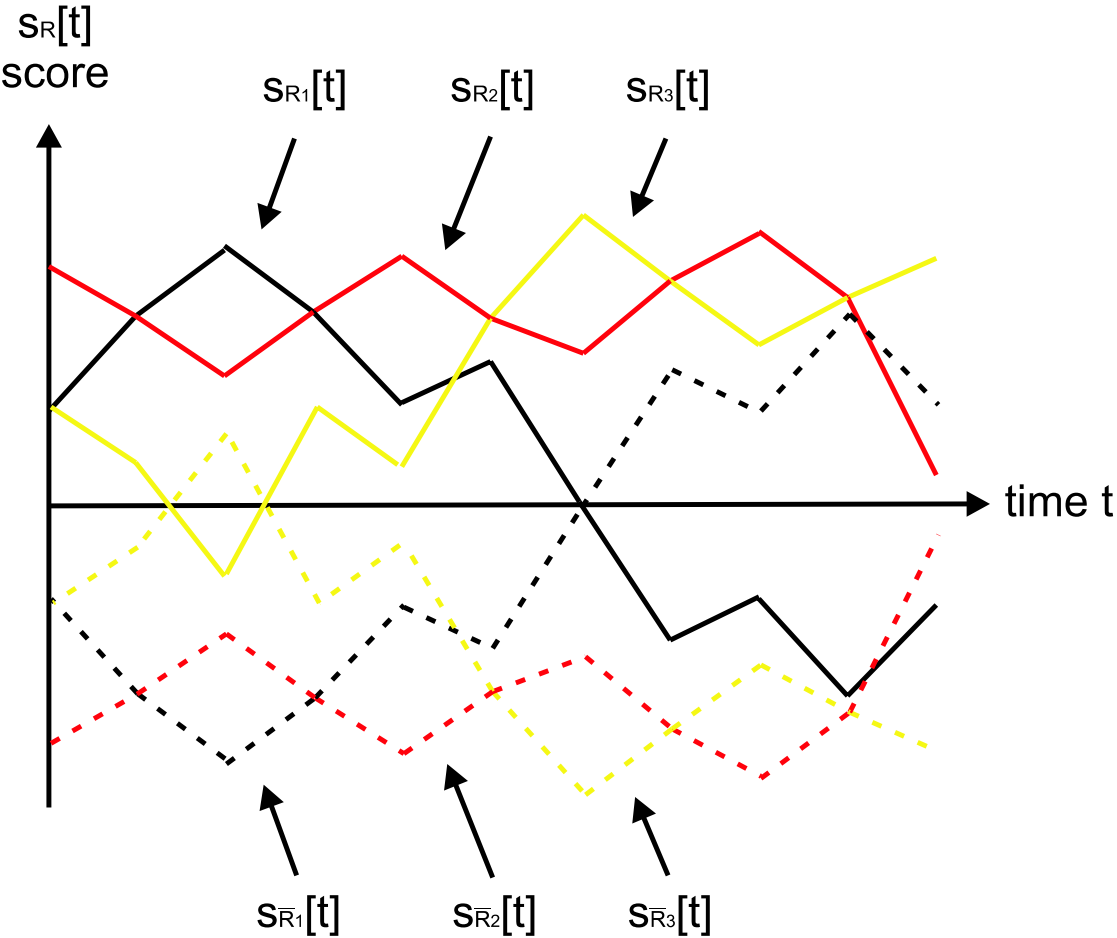


Figure 9

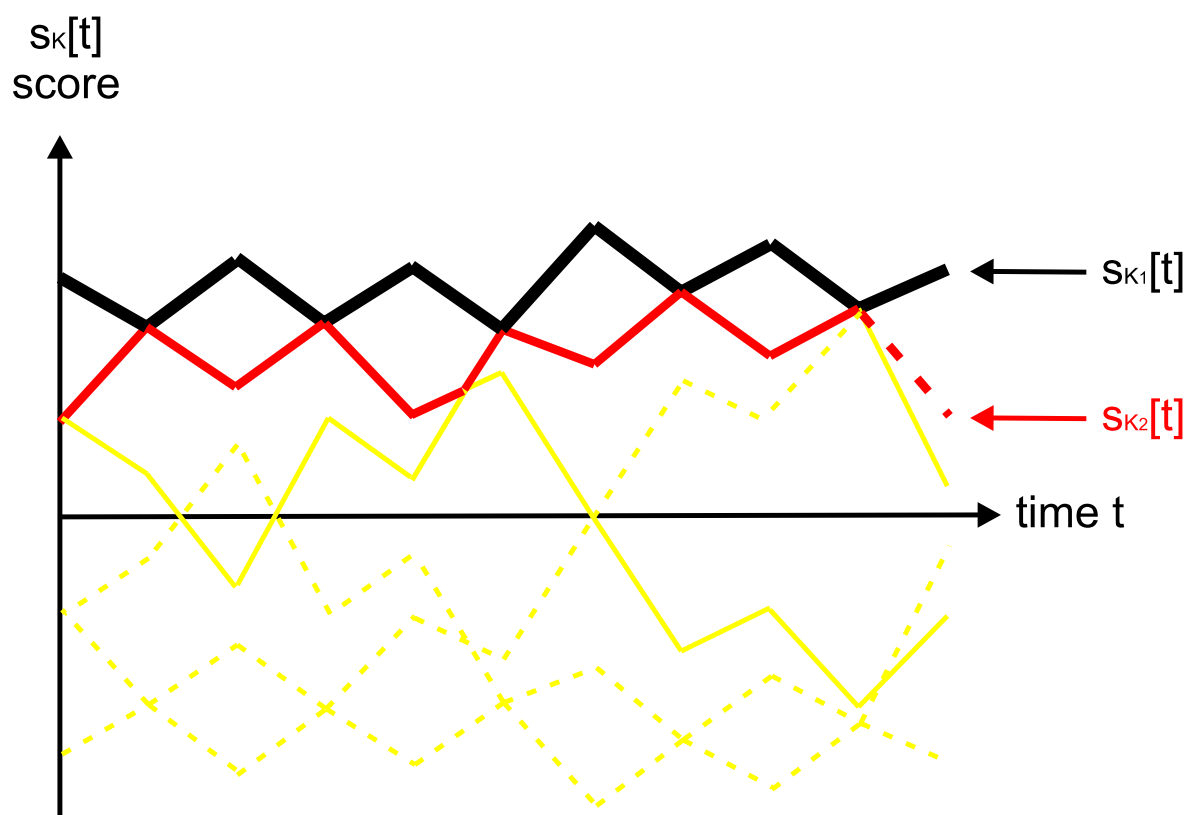


Figure 10

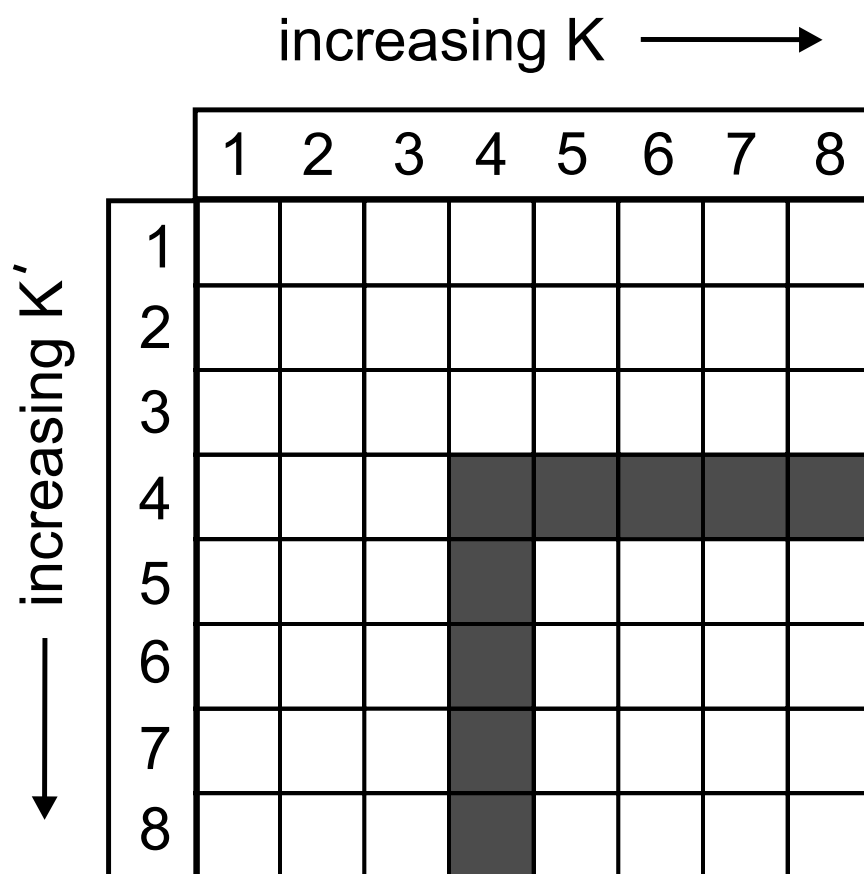


Figure 11

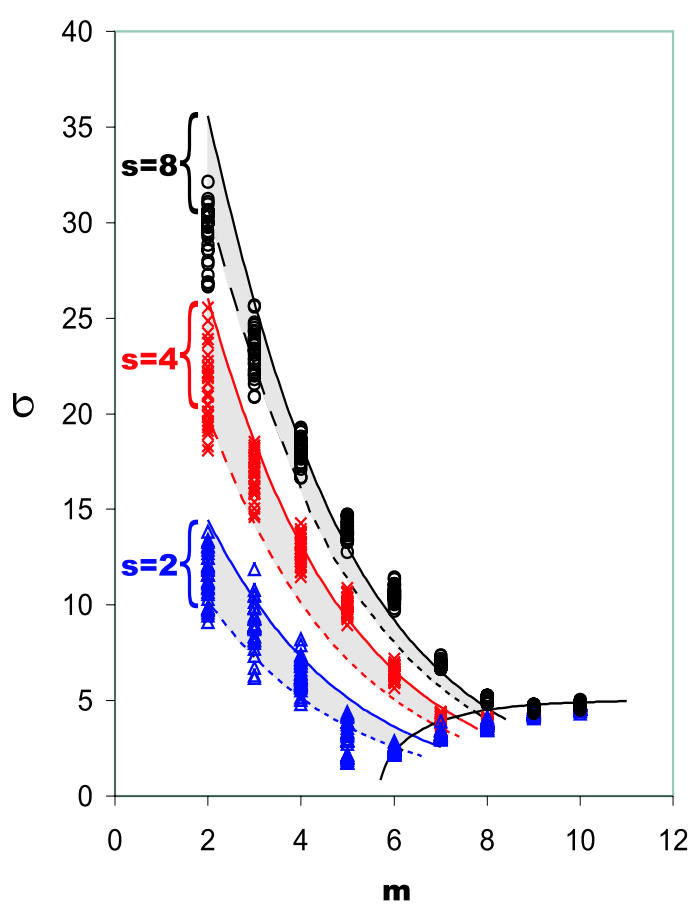


Figure 12

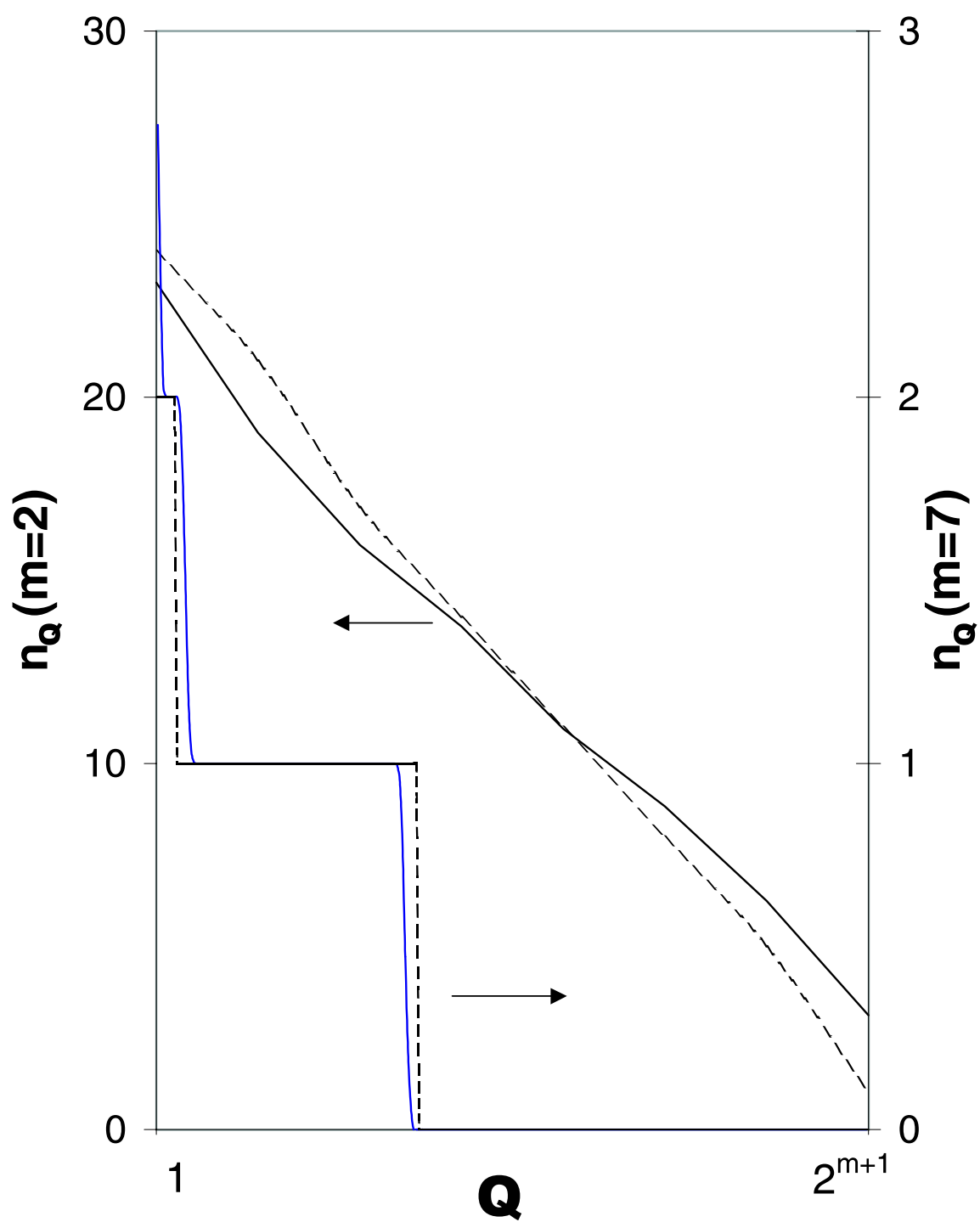


Figure 13

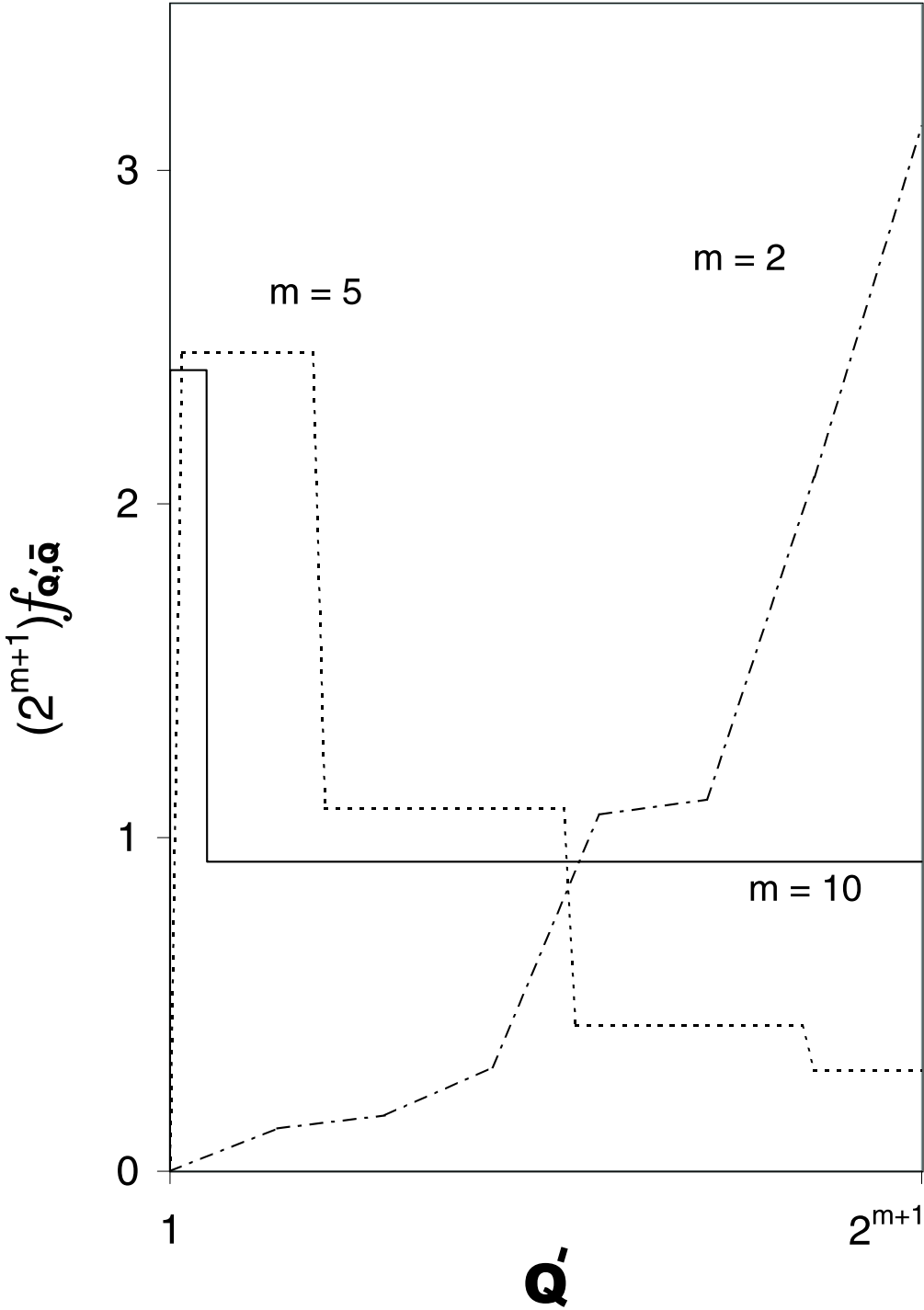


Figure 14

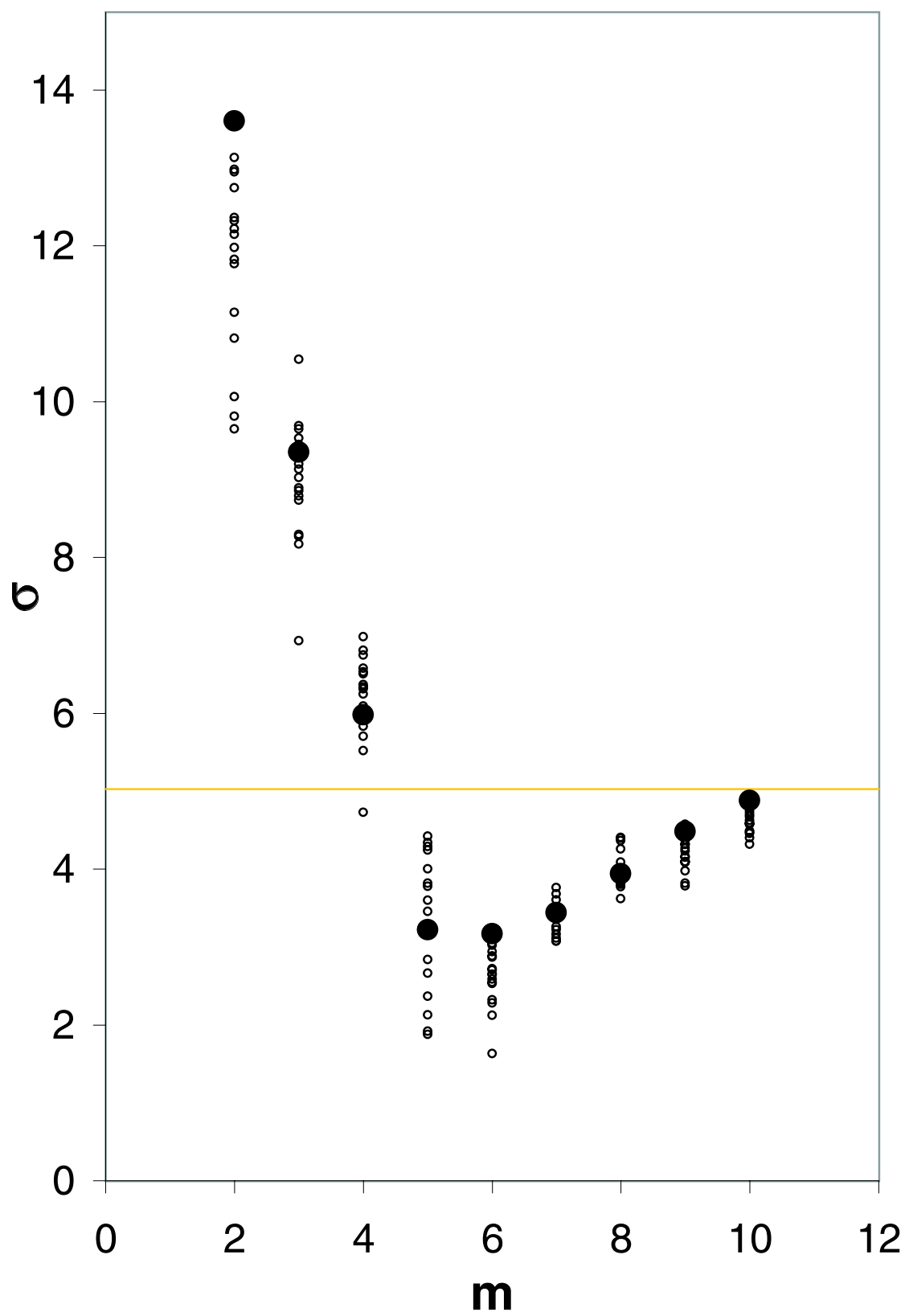


Figure 15

